






## RESEARCH ARTICLE

# Topography of visual and somatosensory inputs to the pontine nuclei in zebra finches (*Taeniopygia guttata*)

Andrea H. Gaede<sup>1</sup>  | Cristián Gutiérrez-Ibáñez<sup>2</sup>  | Pei-Hsuan Wu<sup>3</sup>  |  
Madison C. Pilon<sup>2</sup> | Douglas L. Altshuler<sup>3</sup>  | Douglas R. Wylie<sup>2</sup> 

<sup>1</sup>Structure and Motion Laboratory,  
Department of Comparative Biomedical  
Sciences, Royal Veterinary College, London,  
UK

<sup>2</sup>Department of Biological Sciences, University  
of Alberta, Edmonton, Alberta, Canada

<sup>3</sup>Department of Zoology, University of British  
Columbia, Vancouver, British Columbia,  
Canada

## Correspondence

Douglas R. Wylie, Department of Biological  
Sciences, University of Alberta, Edmonton,  
Alberta, Canada T6G 2E9. Email:  
[dwylied@ualberta.ca](mailto:dwylied@ualberta.ca)

## Funding information

Canadian Institutes of Health Research,  
Grant/Award Number: 159751; Natural  
Sciences and Engineering Research Council of  
Canada, Grant/Award Number: 2018-04976

## Abstract

Birds have a comprehensive network of sensorimotor projections extending from the forebrain and midbrain to the cerebellum via the pontine nuclei, but the organization of these circuits in the pons is not thoroughly described. Inputs to the pontine nuclei include two retinorecipient areas, nucleus lentiformis mesencephali (LM) and nucleus of the basal optic root (nBOR), which are important structures for analyzing optic flow. Other crucial regions for visuomotor control include the retinorecipient ventral lateral geniculate nucleus (GLv), and optic tectum (TeO). These visual areas, together with the somatosensory area of the anterior (rostral) Wulst, which is homologous to the primary somatosensory cortex in mammals, project to the medial and lateral pontine nuclei (PM, PL). In this study, we used injections of fluorescent tracers to study the organization of these visual and somatosensory inputs to the pontine nuclei in zebra finches. We found a topographic organization of inputs to PM and PL. The PM has a lateral subdivision that predominantly receives projections from the ipsilateral anterior Wulst. The medial PM receives bands of inputs from the ipsilateral GLv and the nucleus laminaris precommissuris, located medial to LM. We also found that the lateral PL receives a strong ipsilateral projection from TeO, while the medial PL and region between the PM and PL receive less prominent projections from nBOR, bilaterally. We discuss these results in the context of the organization of pontine inputs to the cerebellum and possible functional implications of diverse somato-motor and visuomotor inputs and parcellation in the pontine nuclei.

## KEYWORDS

avian, lentiformis mesencephali, nucleus of the basal optic root, optic tectum, pons, pretectum, RRID:SCR\_013673, RRID:SCR\_014199, somatosensory Wulst

This is an open access article under the terms of the [Creative Commons Attribution](https://creativecommons.org/licenses/by/4.0/) License, which permits use, distribution and reproduction in any medium, provided the original work is properly cited.

© 2023 The Authors. The *Journal of Comparative Neurology* published by Wiley Periodicals LLC.

## 1 | INTRODUCTION

In mammals, the pontine nuclei receive diverse sensory and motor inputs. These inputs arise not only from visual, somatosensory, motor, and higher-order areas of the cortex but also from subcortical structures such as the inferior colliculus, ventral thalamus, and accessory visual system (Henschke & Pakan, 2020; Kratochwil et al., 2017; Ramnani, 2006). Given the diversity of inputs, it is not surprising that the pontine nuclei have been implicated in a variety of functions, including eye movements, motor planning, and higher cognitive functions (Guo et al., 2021; Nagao, 2004; Ramnani, 2006).

In birds, as in mammals, the pontine nuclei reside at the base of the anterior rhombencephalon, and two subnuclei are clearly visible: the medial (PM) and lateral (PL) pontine nuclei (Figures 1 and 2). Whether these nuclei are homologous to their mammalian counterparts remains unclear (Brodal et al., 1950; Gutiérrez-Ibáñez et al., 2023b). The pontine nuclei of birds project to the cerebellum where is largely restricted to folia VI–VIII, the oculomotor cerebellum (Gutiérrez-Ibáñez et al., 2022). Thus, this projection is much more restricted compared to mammals, where the pontine nuclei project to most of the cerebellum (Biswas et al., 2019; Henschke & Pakan, 2020; Ramnani, 2006). Despite these differences, the pontine nuclei receive similar inputs in both groups. In birds, although there are some species differences (see *Discussion*), the pontine nuclei receive both pallial (cortical) and subpallial input (Wylie et al., 2018). These include inputs from the arcopallium and the Wulst (Dubbeldam et al. 1997; Fernández et al., 2020; Wild & Williams, 2000), ventral geniculate nucleus (GLv) (Marín et al., 2001), optic tectum (TeO) (Hunt & Künzle, 1976; Reiner & Karten, 1982), nucleus of the basal optic root (nBOR) (Wylie et al., 1997), and nucleus lentiformis mesencephali (LM) in the pretectum (Gamlin & Cohen, 1988a) (Figure 1). With respect to this latter projection, Gamlin and Cohen (1988b) suggest that the projection from the pretectum to the PM is not from the LM proper, but from the nucleus laminaris precommisuralis (LPC), which resides immediately medial to LM (see Figure 3)

In mammals, the organization of both cortical and subcortical inputs to the pontine nuclei has been studied in detail in several species. These studies have shown that inputs from different regions of the cortex and subcortical inputs from different sensory modalities are segregated in the pontine nuclei (Giolli et al., 2001; Henschke & Pakan, 2020; Kratochwil et al., 2017; Leergaard & Bjaalie, 2007). In contrast, less is known about the organization of inputs to the pontine nuclei in birds. Previous research suggests that similar to mammals, inputs to the pontine nuclei may be segregated by sensory modality. For example, inputs from the TeO and visual arcopallium are largely restricted to the PL (Fernández et al., 2020; Hunt & Künzle, 1976), whereas inputs from GLv and the somatosensory Wulst are restricted to the PM (Marín et al., 2001; Wild & Williams, 2000). However, more detailed studies are needed. In this study, we examined the topography of inputs to the pontine nuclei in zebra finches (*Taeniopygia guttata*) from pallial and subpallial structures with injections of anterograde tracers in visual (TeO, GLv, LM, nBOR) and somatosensory areas (anterior Wulst). Our

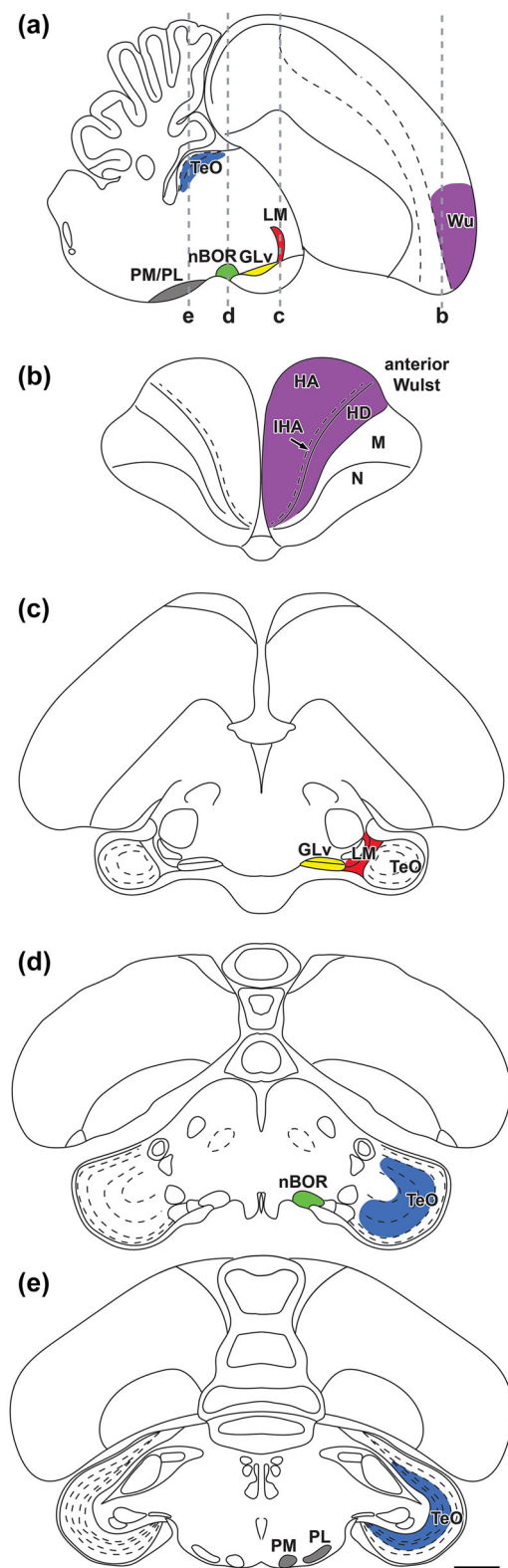


**FIGURE 1** Avian visual motion processing and somatosensory brain areas investigated in the present study. Panel (a) shows an illustration of a parasagittal section through the zebra finch brain indicating the relative locations of structures of interest in this study: the medial (PM) and lateral (PL) pontine nuclei (gray), the optic tectum (TeO; blue); the nucleus of the basal optic root (nBOR; green), the ventral lateral geniculate nucleus (GLv; yellow), the pretectal nucleus

(Continues)

## FIGURE 1 (Continued)

lentiformis mesencephali (LM; red), and the somatosensory anterior Wulst (Wu; purple). Dashed vertical lines in (a) indicate the anterior–posterior locations of the coronal sections shown in (b–e). In the most anterior section, (b), the somatosensory Wulst is indicated in purple. The Wulst is laminated and includes the hyperpallium apicale (HA), the interstitial nucleus of the hyperpallium apicale (IHA), and the hyperpallium densocellulare (HD). Panel (c) illustrates the location of the retinorecipient nuclei GLv (yellow), LM (red), and anterior TeO. Panel (d) shows the nBOR (green) of the accessory optic system and the deep, motion-sensitive layers of the TeO (blue). Panel (e) shows the deep layers of TeO and the medial and lateral pontine nuclei (PM and PL). Other M = mesopallium; N = nidopallium. Scale bar = 1 mm.

results show that visual inputs to the PM and PL are topographically organized and segregated from somatosensory inputs from the anterior Wulst. We discuss our results in relation to the organization of pontine inputs to the cerebellum and possible functional implications, particularly related to the visual control of flight in birds.

## 2 | MATERIALS AND METHODS

### 2.1 | Animals

Eleven adult male zebra finches (*T. guttata*; 13–16 g; L'Oisellerie de L'Estrie) were used for this study (Table 1). All surgical procedures were approved by the University of British Columbia Animal Care Committee in accordance with the guidelines set out by the Canadian Council on Animal Care.

### 2.2 | Surgical procedures

All procedures were performed in birds under surgical anesthesia (65 mg/kg ketamine and 8 mg/kg xylazine; i.m.). Supplemental doses were provided as necessary. Subcutaneous injections of 0.9% saline were administered for hydration. We used a stereotaxic frame designed for small bird neurosurgical procedures (Herb Adams Engineering) to reliably identify the locations of target nuclei for tract tracer injections. First a needle was placed in the stereotaxic tower and the anterior–posterior coordinates of inter-aural zero were obtained. The anesthetized bird was then placed in the stereotaxic frame, secured with the ear bars and a beak bar, such that the angle between the plane passing through the beak bar and ear bars was pitched downward from the horizontal plane by 60°. An incision was made to expose the surface of the skull. As the skull is very thin, the Y-sinus on the dorsal surface of the brain can be seen through the skull. The pitch of the head was then adjusted ( $\pm 5^\circ$ ) such that the junction of the Y-sinus was aligned with the medio-lateral and anterior–posterior coordinates of interaural zero. With this adjustment, the angle between the plane passing through the beak bar and ear bars was pitched downward from the horizontal plane by 55–61°.

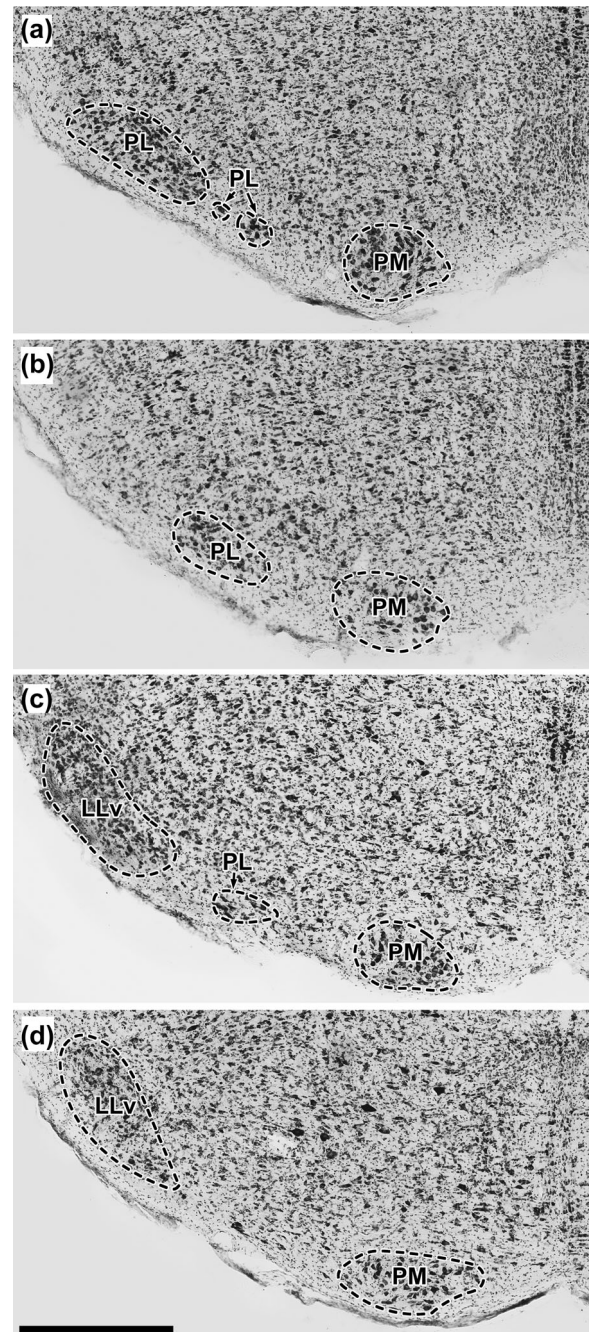


**FIGURE 2** Photomicrographs of Nissl-stained coronal sections through four different levels of the pontine nuclei of the zebra finch from anterior (a) to posterior (d). In a, the lateral pontine nucleus (PL) appears large and shows at least two smaller subdivisions of the ventromedial tail. Panels (b) and (c) show that at more posterior levels, PL becomes progressively smaller. At the most posterior level (d) only the medial pontine nucleus (PM) is visible. Panels (a) and (b) and (c) and (d) are separated by 120 mm. Panels (b)–(c) are separated by 240 mm. LLv = ventral nucleus of the lateral lemniscus. Scale bar = 500  $\mu$ m.

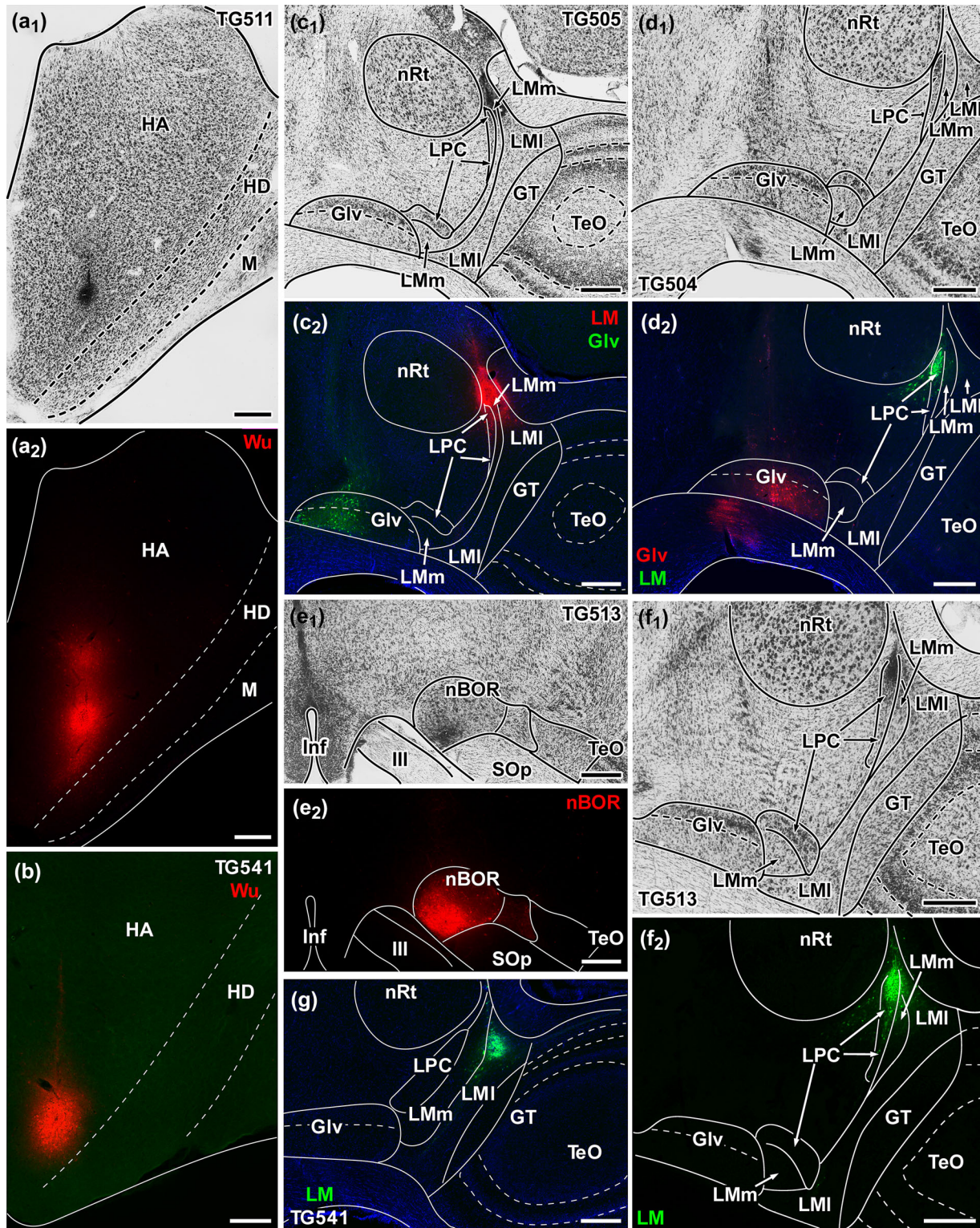


**FIGURE 3** Photomicrographs of coronal sections through injection sites in the somatosensory anterior Wulst (Wu; a and b) and visual structures, nucleus lentiformis mesencephali (LM; c, d, f, and g), the ventral lateral geniculate nucleus (GLv; c and d), and the nucleus of the basal optic root (nBOR; e). With the exceptions of (b) and (g), both fluorescent images (a<sub>2</sub>, c<sub>2</sub>, d<sub>2</sub>, e<sub>2</sub>, and f<sub>2</sub>) and Nissl-stained images of the same sections are shown (a<sub>1</sub>, c<sub>1</sub>, d<sub>1</sub>, e<sub>1</sub>, and f<sub>1</sub>). The case numbers associated with each injection are indicated. The injection target is indicated in the corner of fluorescent images, and color of text indicates the color of dextran used. In panels (a) and (b), both injections were localized in the hyperpallium apicale (HA) of the somatosensory Wulst. The medial and lateral subnuclei of LM are indicated (LMm, LMI). The injections in LM involved the medial and lateral subnuclei (LMm, LMI), as well as the adjacent nucleus laminaris precommissuralis (LPC), which lies medial to LMm and projects to the oculomotor cerebellum in zebra finches (Gaede et al., 2019). See text for a more detailed description of the extent of each LM injection. The

(Continues)

**FIGURE 3** (Continued)

dashed line through the GLv represents the border between the internal and external laminae (c and d). Other HD, hyperpallium densocellulare; M, mesopallium; nRt, nucleus rotundus; GT, tectal gray; III, third cranial nerve; Inf, infundibulum; SOp, stratum opticum. All scale bars = 250  $\mu$ m.

**TABLE 1** A case list of injections of anterograde tracers into visual and somatosensory structures of the zebra finch. For each case, the target injection for Texas red (red) and/or fluorescein (green) conjugated dextrans is/are indicated. Targets included the anterior somatosensory Wulst, nucleus lentiformis mesencephali (LM), ventral lateral geniculate nucleus (GLv), nucleus of the basal optic root (nBOR), and the optic tectum (TeO). Photomicrographs of the injections appear in Figures 3 and 4 as indicated. All injections were on the right side of the brain.

Case	Red injection	Green injection
TG511	Wulst (Figure 3a)	
TG541	Wulst (Figure 3b)	LM (Figure 3g)
TG505	LM (Figure 3c)	GLv (Figure 3c)
TG504	GLv (Figure 3d)	LM (Figure 3d)
TG513	nBOR (Figure 3e)	LM (Figure 3f)
TG496	LM (Figure 4a)	
TG502	LM (Figure 4b)	nBOR (Figure 4c)
TG503	nBOR (Figure 4e)	LM (Figure 4d)
TG497	nBOR (Figure 4f)	
TG499	TeO (Figure 4h)	LM (Figure 4g)
TG516	TeO (Figure 4i)	nBOR (Figure 4i)

We performed a small craniotomy over the target region so that micropipettes lowered in the vertical plane could reach the LM, nBOR, GLv, TeO, or anterior Wulst. To confirm location in the intended visual or somatosensory nucleus, we recorded extracellular activity from single units in response to relevant sensory stimuli; namely, visual motion (e.g., large-field dot patterns, light flash) or touch (e.g., feather deflection, brushing, tapping). For this, we lowered glass micropipettes filled with 2 M NaCl (tip diameter  $\sim$ 20  $\mu$ m) using an electric microdrive (Frederick Haer & Co.). Extracellular signals were amplified and filtered (A-M Systems Model 3000) prior to being digitized (Cambridge Electronic Design; micro 1401-3). For the LM and nBOR, once a cell was isolated, we qualitatively determined the direction preference of the unit by moving a handheld visual stimulus (90°  $\times$  90°), comprised of

black lines and dots on a white background, in multiple directions at a range of speeds within the cell's receptive field as previously described (Gaede et al., 2017; Pakan et al., 2010; Smyth et al., 2022; Wylie et al., 2023). For the TeO and GLv, we identified injection sites by selecting those with the most robust response to a light flash. We identified cells in the somatosensory Wulst using a paintbrush to tap and brush regions of the body. Once an injection site was confirmed with recording, we retracted the recording pipette, removed the saline solution, and refilled it with a fluorescent conjugated dextran (10% in 10 mM PBS), either Texas red (D3328; 3000 molecular weight; Invitrogen by Thermo Fisher Scientific) or fluorescein (D3306; 3000 molecular weight; Invitrogen by Thermo Fisher Scientific). We then lowered the micropipette to the recording site and injected the dextran via iontophoresis ( $\pm$ 4.5  $\mu$ A; 7 s on, 7 s off) for 15–40 min, followed by 5 min of rest prior to removing the micropipette. In several cases, recordings and injections were performed in a second target nucleus using a new micropipette with a tracer of the opposite color. At the end of the surgery, we used bone wax to seal the craniotomy and the incision was sutured with cyanoacrylate (Vetbond; 3 M).

### 2.3 | Brain extraction and sectioning

We recovered the birds for 4 days to allow bidirectional transport of the tracers. The birds were then deeply anesthetized with ketamine/xylazine (i.m.) transcardially perfused with 0.9% NaCl, followed by 4% paraformaldehyde (PFA) in 0.1 M PBS (pH 7.4). Brains were removed from the skull and stored in 4% PFA overnight at 4°C. They were then transferred to 30% sucrose in 0.01 M PBS until they sank, which cryoprotects the tissue for sectioning. Next, we embedded the brains in gelatin and cryoprotected the block in 30% sucrose again. Brains were sectioned using a freezing microtome into three series in the coronal plane at a thickness of 40  $\mu$ m. The sections were mounted on gelatinized glass slides, dried, and stored at 4°C. To aid alignment of fluorescent and brightfield images and the delineation of pretectal nuclei borders, a few drops of SlowFade Gold antifade reagent with DAPI (Invitrogen) was applied to sections through the pons and pretectum as previously described (Gutiérrez-Ibáñez et al., 2018; Wylie et al., 2023).

### 2.4 | Microscopy and image analysis

To acquire images of injection sites, terminal labeling in the pontine nuclei, and terminal or soma labeling in other sites, we applied a few drops of PBS to the slides and temporarily cover-slipped them. We viewed sections using a compound light microscope (Leica DM6B) equipped with TX2 (red), L5 (green), and DAPI (blue) fluorescent filters. Images were captured with a K5 (Leica) camera using Leica Application

Suite X imaging software (RRID:SCR\_013673). We used Adobe Photoshop (RRID:SCR\_014199) to compensate for brightness and contrast. After acquiring all fluorescent images, we removed the coverslips and dried the slides for storage or subsequent Nissl staining with thionin. In short, slides were air dried, hydrated through a graded series of ethanol solutions, stained for 3 min in a 0.2 % thionin solution in a 4.4 pH acetate buffer, then dehydrated through a graded series of ethanol solutions, cleared in Citrasolv (Fisher Scientific), and cover-slipped in Permount (Fisher Scientific).

Images were then taken of the Nissl-stained sections and these were overlaid upon the fluorescent images of the same sections. This allowed for an accurate delineation of the borders of brain nuclei to determine the precision of the injections in targeted sites, and to more accurately illustrate the topography of projections to the PM and PL.

## 2.5 | Divisions of PL and PM

The extent of the boundaries of PM and PL are shown in Nissl sections in Figure 2. At more anterior levels, PL appears large, and there appear to be two separate regions: the bulk of the nucleus is dorsolateral (Figure 2a) while one or two small clusters of cells reside ventromedially (Figure 2a). At more posterior levels, PL is smaller and located more medially (Figures 2b and c). PM appears as a single mass of cells that continues posterior to PL (Figure 2d).

## 3 | RESULTS

### 3.1 | Injection sites

The eleven cases used in this study are summarized in Table 1. Eight cases received injections in two sites allowing us to visualize the topography of projections from both nuclei simultaneously, while three cases received a single injection. Injection sites for all cases are shown in Figures 3 and 4. Figure 3a serves as an example to illustrate the methods used to localize injection sites. We first obtained a fluorescent image (Figure 3a2), subsequently Nissl-stained the section (Figure 3a1), and finally used the overlay to draw the boundaries of key structures on the fluorescent image (Figure 3a2).

Two cases received injections in the anterior somatosensory Wulst (Figures 3a and b). Likewise, there were two injections into the GLv, with one placed medially (Figure 3c) and the other more laterally (Figure 3d). Five cases included injections confined to the nBOR (Figures 3e and 4c, e, f, and i) and two cases received injections targeting the deep layers of the TeO (Figures 4h and i).

The LM was injected in eight cases. The LM is a crescent-shaped structure in the pretectum that consists of medial and lateral subnuclei (LMm, LMI), both of which are retinorecipient (Gamlin & Cohen, 1988b). Internal to LMm is the nucleus LPC which consists of densely packed neurons, the dendrites of which extend into LMm (Vega-Zuniga et al., 2016). Of the eight LM injections, three were found in the rostral half of the pretectum. Two of these three were largely confined to

LMI (cases TG496, TG503; Figures 4a and d) and one was largely confined to LMm (case TG502; Figure 4b). The other five injections were located dorsally in the caudal half of LM. In case TG541, the injection was confined to LMI (Figure 3g). In case TG505, the injection was in the extreme dorsal part of LM, where the borders of the subnuclei are difficult to distinguish. It appeared to include LMm, LMI, and the adjacent LPC (Figure 3c). In cases TG504 and TG513, the injections were largely confined to LPC, with some spread to the adjacent LMm (Figures 3d and f). Last, in case TG499 the injection involved both the LPC and LMm (Figure 4g).

### 3.2 | Connections of the anterior Wulst, GLv, LM, nBOR, and TeO in zebra finches

Although the focus of this article is the projections to the pontine nuclei, we note that from our injections we found anterograde and retrograde labeling consistent with previous studies in zebra finches and other birds. Injections into the anterior Wulst resulted in retrograde labeling in the nucleus dorsalis intermedialis ventralis anterior of the dorsal thalamus (Figure 5a). From both cases with injections in the Wulst, anterograde labeling was not observed in the TeO or GLv, confirming that our injection was confined to the anterior somatosensory Wulst and spared the posterior visual Wulst (Funke, 1989; Schneider & Necker, 1996; Wild, 1987, 1997; Wild et al., 2008; Wild & Williams, 2000). Injections into the GLv led to retrograde labeling of characteristic “vine” neurons in layer 10 of the TeO (Figures 5b and c). These neurons can be recognized by their radial morphology, dense dendritic branching in layer 7 of the TeO, and an axon that travels through the upper tectal layers and makes a 90° turn in the optic tract (Figure 5c). Injections in GLv also resulted in anterograde labeled terminals in the tectal gray (GT; Figure 4b) (Vega-Zuniga et al., 2016).

From injections in the LM, we observed terminals in the ipsilateral nBOR pars dorsalis (nBORd; Figure 5d) and mossy fiber rosettes clustered in parasagittal stripes in the granular layer of folia VI-IXcd of the cerebellum (Figure 5e). LM injections also retrogradely labeled some nBOR cells (Figure 5d) and nBOR injections resulted in strong terminal labeling in the LM (Figure 5f). Together these results illustrate reciprocal connections between the LM and nBOR, as previously described in pigeons and zebra finches (Brauth & Karten, 1977; Brecha et al., 1980; Brecha & Karten, 1979; Clarke, 1977; Gamlin & Cohen, 1988a; Wylie et al., 2023). LM and nBOR terminals bilaterally targeted the inferior olive (IO), though heavier on the side ipsilateral to the injection site and demonstrated distinct topographical projections in the medial column of the IO (Figure 5g) (Pakan et al., 2010; Wylie et al., 2023). Injections in the TeO produced extensive anterograde and retrograde labeling consistent with those previously reported in pigeons and other birds (Faunes et al., 2013; Gamlin et al., 1996; Hellmann & Güntürkün, 2001; Hunt & Künzle, 1976; Luksch, 2003; Reiner & Karten, 1982; Wang et al., 2006). For example, retrograde labeling of large cells in the nucleus isthmi pars magnocellularis (Imc; Figure 5h) as well as a locus of terminal labeling and retrogradely labeled cells in the nucleus isthmi pars parvocellularis (Ipc; not shown). Shown in Figure 5i, from

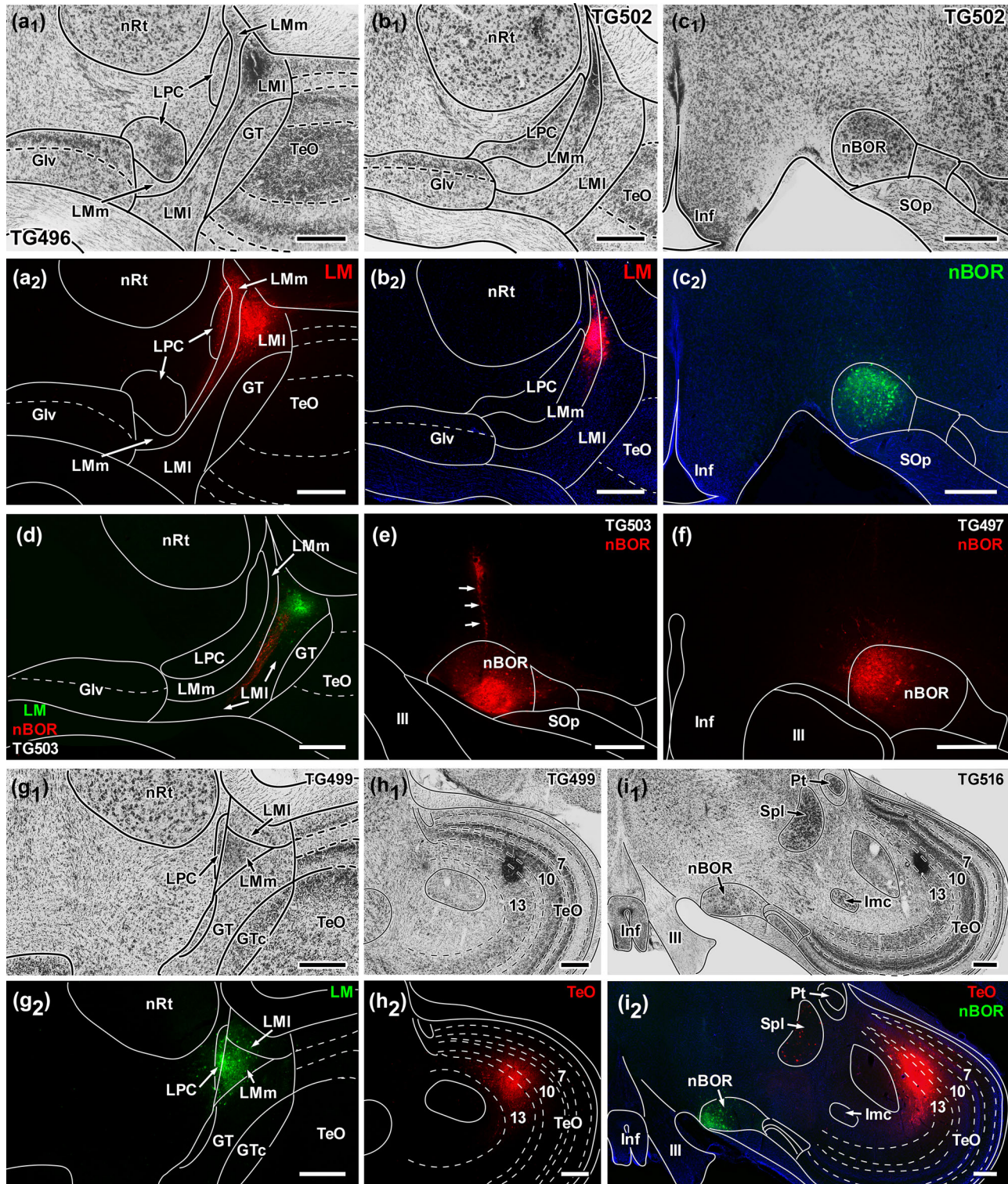


**FIGURE 4** Photomicrographs of coronal sections through injection sites in the pretectal nucleus lentiformis mesencephali (LM; a, b, d, and g), the nucleus of the basal optic root (nBOR; c, e, f, and i), and the optic tectum (TeO; h and i). With the exceptions of d, e, and f, both fluorescent images (a<sub>2</sub>, b<sub>2</sub>, c<sub>2</sub>, g<sub>2</sub>, h<sub>2</sub>, and i<sub>2</sub>) and Nissl-stained images of the same sections are shown (a<sub>1</sub>, b<sub>1</sub>, c<sub>1</sub>, g<sub>1</sub>, h<sub>1</sub>, and i<sub>1</sub>). The case numbers associated with each injection are indicated. The injection target is indicated in the corner of fluorescent images, and color of text indicates the color of dextran used. The injections in LM involved the medial and lateral subnuclei (LMm, LMI), as well as the adjacent nucleus laminaris precommissuralis (LPC), which lies medial to LMm and projects to the oculomotor cerebellum in zebra finches (Gaede et al., 2019). See text for a more detailed description of the extent of each LM injection. The dashed line through the ventral lateral geniculate nucleus (GLv) represents the border between the internal and external laminae (a, b, and d). In d, the red terminals in LMI arise from the injection in nBOR shown in e. The white arrows in e indicate the micropipette track above nBOR. The numbered layers of the optic tectum are indicated in h and i (7, 10, 13) to emphasize that the injections were in the deeper layers (10, 13). Other nRt, nucleus rotundus; GT, tectal gray; GTc, tectal gray pars compacta; III, third cranial nerve; Inf, infundibulum; SOp, stratum opticum; Spl, lateral spiriform nucleus; Pt, nucleus pretectalis; Imc, nucleus isthmi pars magnocellularis. All scale bars = 250  $\mu$ m.

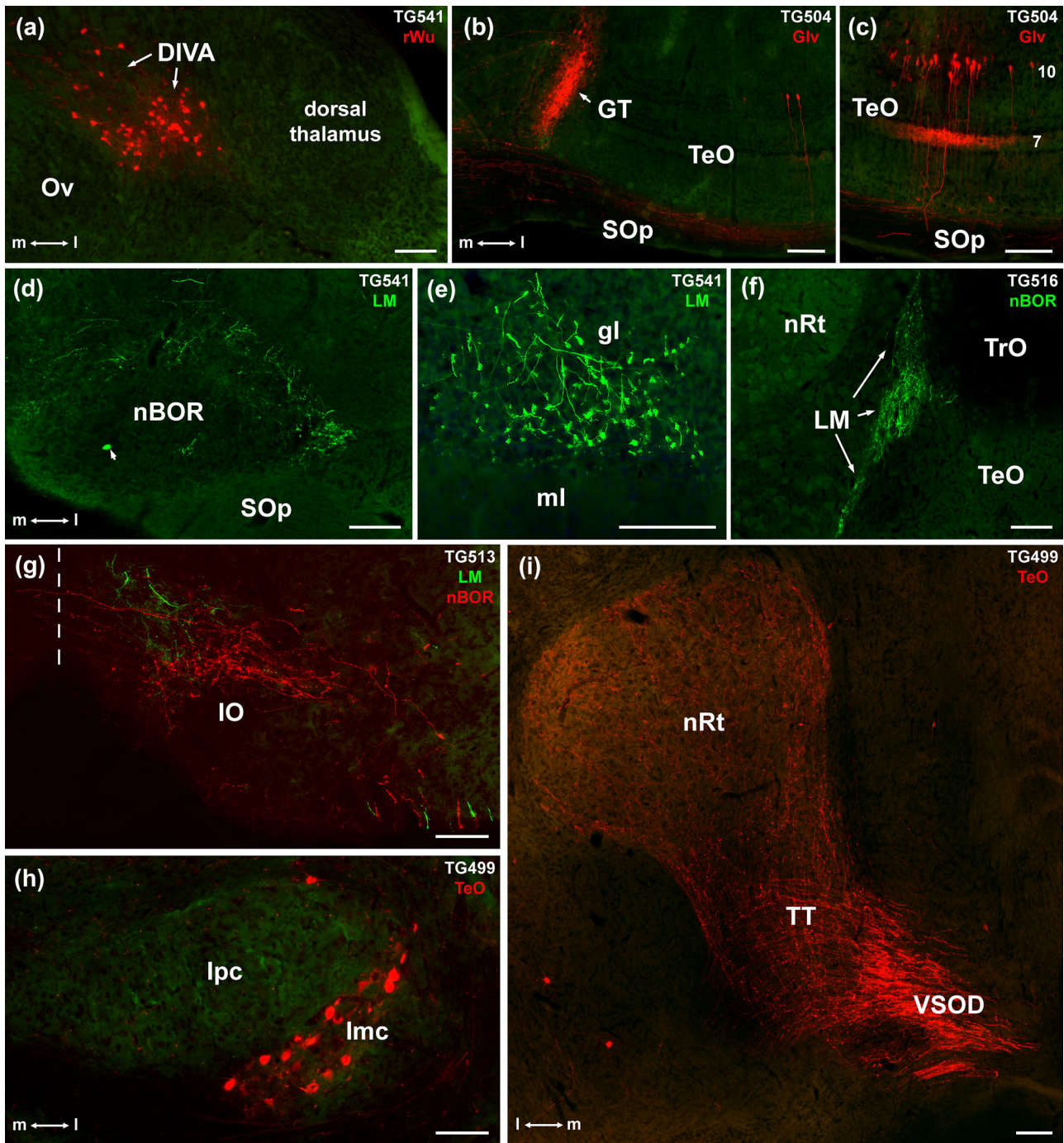


**FIGURE 5** Fluorescence photomicrographs of anterograde and retrograde labeling from injections in the somatosensory Wulst, ventral lateral geniculate nucleus (GLv), nucleus lentiformis mesencephali (LM), nucleus of the basal optic root (nBOR), and the optic tectum (TeO). For each panel the case is indicated as well as the target of the injection and the color of dextran (red or green) injected. Panel (a) shows a photomicrograph of retrograde labeling in the nucleus dorsalis intermedius ventralis anterior (DIVA) of the dorsal thalamus from injection in the anterior Wulst. From injections in GLv, panel (b) shows anterograde labeled terminals in the tectal gray (GT) and panel (c) shows retrograde labeling of "vine" neurons in layer 10 of the TeO. (d and e) From injections in LM, panels (d) and (e) show, respectively, terminal labeling in the ipsilateral dorsal part of nBOR and mossy fiber rosettes in the granular layer (gl) folium IXcd of the cerebellum. In panel (d), note the retrogradely labeled neuron in nBOR (white arrow). Panel (f) shows anterograde labeling in the LM from an injection in the nBOR. g shows anterograde labeling medially in the inferior olive (IO) from injections in nBOR and LM. The vertical dashed line indicates the midline. Last, injection in the TeO resulted in retrogradely labeled cells in the nucleus isthmi pars magnocellularis (Imc; h) and anterogradely labeled fibers traveling via the tecto-thalamic tract (TT) and terminating diffusely and bilaterally in the nucleus rotundus (nRt). Other ml, molecular layer of cerebellum; TrO, optic tract; lpc, nucleus isthmi pars parvocellularis; Ov, nucleus ovoicalis; SOp, stratum opticum; VSOD, ventral supraoptic decussation. All scale bars = 100 μm.



the TeO, a large bundle of fibers traveled via the tecto-thalamic tract (TT) to nucleus rotundus (nRt).

### 3.3 | Topography of projections to the pontine nuclei

A topographic projection of terminal labeling was observed in the pontine nuclei from injections in the somatosensory Wulst and visual nuclei. These data are shown in Figures 6–9. Figures 6–8 show photomicrographs for these cases, whereas Figure 9 shows drawings of serial sections through the pontine nuclei from rostral to caudal.

#### 3.3.1 | Projections from the somatosensory Wulst

Photomicrographs of terminal labeling in the pontine nuclei from the injections in the anterior Wulst are shown in Figure 6ab, and drawings of terminal labeling throughout the rostro-caudal extent are shown in Figure 9d. Heavy terminal labeling was restricted to the dorso-lateral region of the medial pontine (Figures 9d<sub>2–7</sub>). In Nissl-stained sections, this region usually appeared as a subnucleus of more densely packed cells with a separation from the ventro-medial region (e.g., Figures 6a<sub>1</sub>, f<sub>1</sub>, g<sub>1</sub>, 7b<sub>1</sub>, 8b<sub>1</sub>, and c<sub>1</sub>). Moreover, this dorso-lateral region of PM was generally devoid of labeling from injections in the visual nuclei (e.g., Figures 6d, f<sub>2</sub>, g<sub>2</sub>, and 8c<sub>2</sub>; see below for description). From the anterior Wulst injections, some lighter terminal labeling was observed amongst the labeled fibers surrounding PM, particularly medial to PM (Figures 6a<sub>2</sub>, b, and 9d<sub>2–9</sub>).

#### 3.3.2 | Projections from the GLv

Photomicrographs of terminal labeling in PM from injections in GLv are shown in Figures 6c–e and drawings of serial sections through the pontine are shown for case TG505 in Figure 9c. The terminals from GLv were very fine in appearance. Although terminals could be seen over much of PM, terminal labeling was extremely heavy and dense in a central region with sparing medially and dorsolaterally (Figure 9c<sub>2–6</sub>). To reiterate, the dorso-medial region labeled from injections in the Wulst (described above), was sparsely labeled from injections in GLv (Figures 6d and 9c<sub>2–6</sub>). The region of sparse labeling medial to the central region containing GLv terminals, was more heavily labeled from injections in LM (e.g., Figure 6d; see below). The terminal labeling from GLv persisted quite caudally, where the posterior end of PM is very small (Figures 6e and 9c<sub>9–13</sub>). This posterior region received little labeling from injections in other pontine-projecting nuclei (Figure 9).

#### 3.3.3 | Projections from LM

The projections from the LM to the pontine were quite variable and related to the location of the injection in the pretectum. Labeling was seen across the medial pontine from four cases in particular: TG504,

TG505, TG513, and TG499. As described above, in these cases the injections were centered on LPC, or at least included, LPC. From these cases the labeling was seen in PM, with a ventro-medial emphasis (Figures 6d, f, g and 8, 9b, c, and e). Critically, the terminal labeling was largely absent from the dorso-lateral area of the PM that receives input from the anterior Wulst (Figures 6d, e, g, 8c, and 9b<sub>3–5</sub>, c<sub>3–7</sub>, e<sub>2–6</sub>). This LM labeling also appeared heavier more medial to the central region of PM that contained terminals from GLv (e.g., Figure 6c), but there was certainly some overlap in the projections from GLv and the pretectum (Figure 9c).

From all eight LM cases, including those where the injection was largely confined to LMI and spared LPC, labeled fibers were observed passing through the ventro-medial tail of PL and the interstitial region between PM and PL (Figures 9b<sub>2–7</sub>, c<sub>1–5</sub>, and e<sub>1–6</sub>). In the photomicrographs, terminals are clearly visible amongst these fibers both in the interstitial region and the tail of PL (Figures 6c–g, 7a–c, and 8). Labeled fibers from the LM injections would continue caudally lateral to PM as part of the descending pretectal tract (Dpt; Figures 9b and e). Terminals could be seen amongst these fibers between the caudal part of PM and medial to the spinal lemniscus. At more posterior levels, fibers and terminals can be seen more dorsally, in the trapezoid body (CTz) (Karten & Hodos, 1967) and parts of the reticular formation (Figures 9b<sub>7–12</sub> and 9e<sub>5–13</sub>).

#### 3.3.4 | Projections from nBOR

In all cases with injections in nBOR, fibers traveled in the same place as those from LM injections, passing through the ventro-medial tail of PL and the region between PM and PL (Figures 6f, 7b, 9a, and 9e), in the descending pretectal tract. Similar to LM projections, terminals are also clearly visible amongst these fibers both in the interstitial region and the tail of PL (Figures 6f, 7b, 9a, and 9e). Some fibers traveled dorsal and medial to the ipsilateral PM, through the CTz, then crossed the midline, and could be seen in the contralateral side, around PM and VI nerve in the contralateral CTz (Figures 7e and 9a). Terminals could also be seen in the ipsilateral and contralateral PM, but these were few in number and disparate (Figures 6f, 7b, c, and e).

#### 3.3.5 | Projections from TeO

Both TeO injections (TG 499, TG 516) resulted in labeling of the ipsilateral tectopontine–tectoreticular (ITP) and the crossed tectobulbar pathways, as in pigeons (Reiner & Karten, 1982). The ITP appears as a massive bundle of fibers that can be seen coursing ventrally through the lateral most part of the rostral pons (Figure 8a). At rostral levels, this bundle of fibers leaves large and dense terminals in the PL and the medially adjacent lateral mesencephalic reticular formation (Figures 6g, 8a, and 9b<sub>1–4</sub>). The fibers continue ventromedially towards PM and terminate around and inside the medial subdivision of PM (Figures 8b and c and 9b<sub>3–6</sub>), although these terminals are not as dense as those in PL. Despite the strong labeling of the cross tectobulbar pathways, which send projections to the contralateral side of the brain,

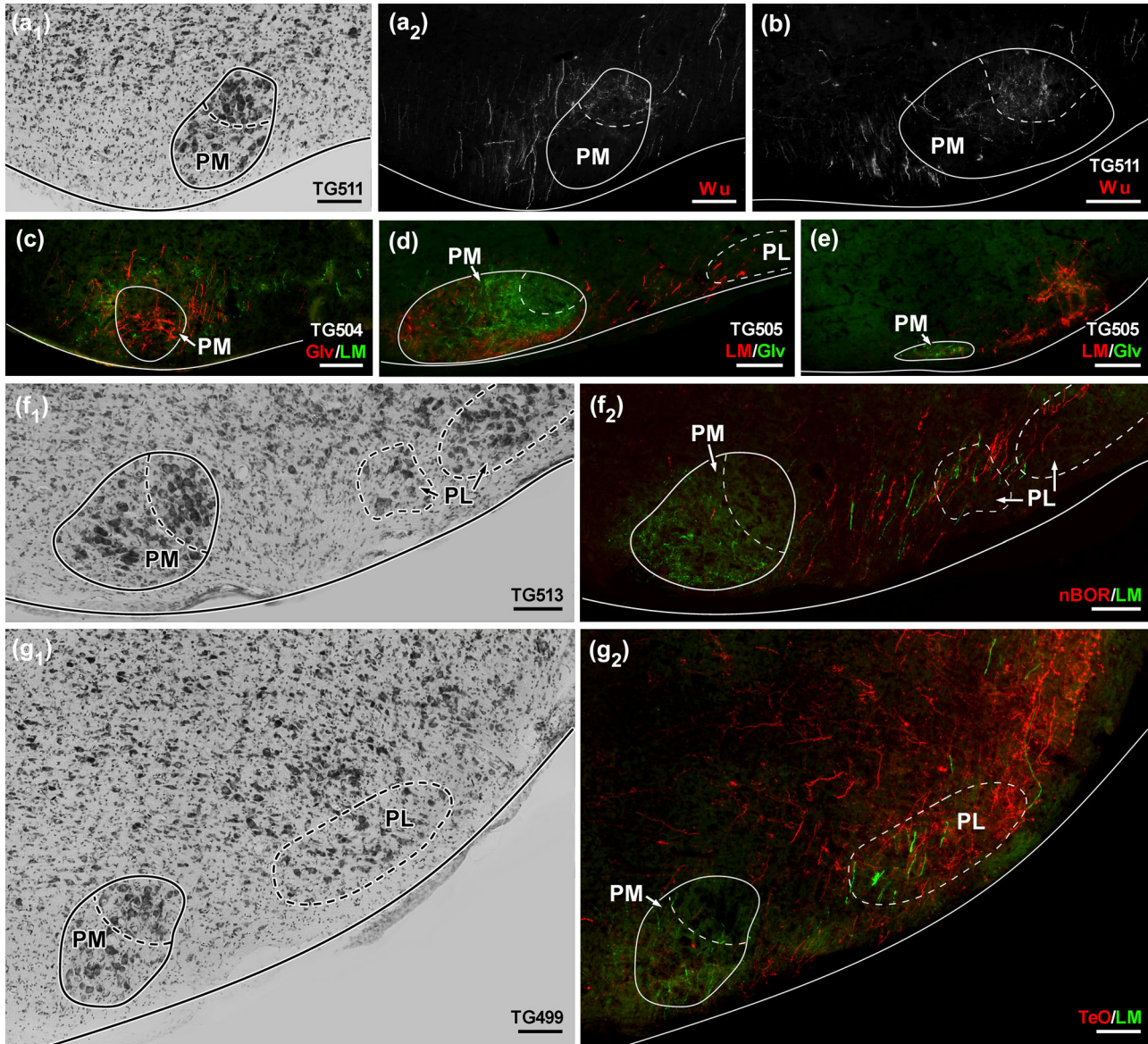


**FIGURE 6** Photomicrographs of terminal labeling in the pontine nuclei from injections of anterograde tracers in visual and somatosensory brain regions. Nissl-stained coronal sections were used for identifying the borders and subdivisions of the pontine nuclei. The case ID and injection target are indicated in the bottom right corner of photomicrographs. The color of the dextran injected is indicated by text color. (a<sub>1</sub>) A Nissl-stained section from TG511 showing the borders of the medial pontine nucleus (PM), including a lateral subregion consisting of a cluster of intensely labeled, closely packed cells. (a<sub>2</sub>) The corresponding fluorescent image showing anterogradely labeled terminals from an anterior Wulst (Wu) injection aligning with the lateral subregion of PM; separation of medial and lateral subregions indicated by dashed line. (b) Fluorescent photomicrograph of a coronal section posterior to (a<sub>2</sub>); anterior Wulst terminals are visible in the lateral subregion of PM. (c) Terminal labeling in the anterior PM from an injection in the ventral lateral geniculate nucleus (GLv). (d) Bands of terminal labeling in medial PM from an injection in the lentiformis mesencephali (LM)/ nucleus laminaris precommissuralis (LPC) and lateral PM from an injection in GLv. (e) In a more posterior section of the same case shown in (d), terminal labeling from a GLv injection is visible throughout PM. (f<sub>1</sub> and f<sub>2</sub>) A Nissl-stained section (f<sub>1</sub>) was used to determine the boundaries of PM and PL, which were overlaid on the corresponding fluorescent image of terminal labeling in the same section (f<sub>2</sub>). In this section, PL is separated into two divisions that are outlined using dashed lines. In panel (f<sub>2</sub>), anterograde terminal labeling from an LM injection fills the medial subdivision of PM and a few en passant fibers pass through the medial division of PL. In the same case (TG513), nucleus of the basal optic root (nBOR) fibers pass between the PM and PL and overlap with LM fibers in the medial division of PL. (g<sub>1</sub> and g<sub>2</sub>) Corresponding Nissl-stained and fluorescent photomicrographs showing strong terminal labeling in the PL from an injection in the optic tectum (TeO) and terminal labeling from an LM/LPC injection similar to (f<sub>2</sub>). Scale bars = 100 μm.

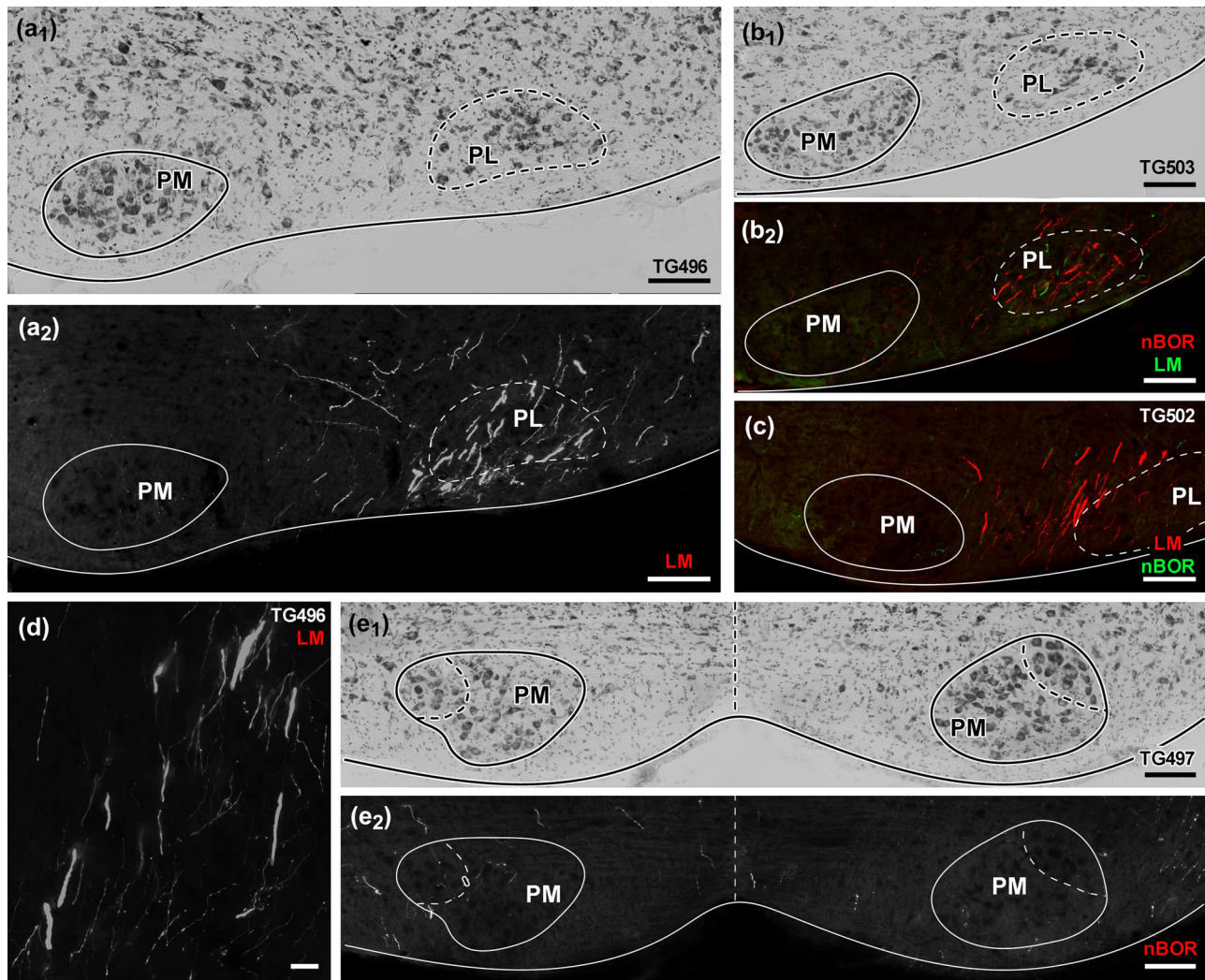


**FIGURE 7** Photomicrographs of terminal labeling in the medial and lateral pontine nuclei (PM and PL) from injections of anterograde tracers in the lentiformis mesencephali (LM) and nucleus of the basal optic root (nBOR). The case ID and injection target are indicated in the corner of photomicrographs. The color of the dextran injected is indicated by text color. (a<sub>1</sub>) A Nissl-stained coronal section showing the borders of PM and PL at the level where PL is first visible. Borders are overlaid in white on the corresponding fluorescent image in panel (a<sub>2</sub>) showing LM fibers passing through PL. (b<sub>1</sub> and b<sub>2</sub>) Nissl-stained section and corresponding fluorescent photomicrographs showing PM and PL borders and LM and nBOR fibers traveling through PL. Panel (c) shows LM fibers passing between PM and PL and fine nBOR terminals in PM. (d) A high magnification image of LM fibers with collateral terminals. (e<sub>1</sub> and e<sub>2</sub>) Bilateral projections of anterogradely labeled fibers from the right nBOR to PM. Scale bars: d = 25  $\mu$ m; all others 100  $\mu$ m.

no terminals were observed in the contralateral PL or PM (data not shown). At more posterior levels, the fibers from TeO course medial and ventral to LLv, with terminals apparent in the reticular formation and CTz adjacent to PM (Figures 8b and 9 b<sub>6-12</sub>).

#### 4 | DISCUSSION

In this study, we delineated the topography of projections from visual and somatosensory brain regions to the pontine nuclei of zebra finches. We show that projections from regions responding to optic flow (LM and nBOR), local visual motion (TeO and GLv), and somatosensory stimuli (anterior Wulst) form a topographic map in PM. This is sum-

marized in Figure 10. The anterior Wulst, GLv, and LM project to the dorsolateral, central, and ventromedial regions of PM, respectively. The boundaries of these projections are not distinct and there are some regions receiving overlapping projections. As discussed below, the projection to the ventromedial part of PM is more likely from LPC rather than LM proper. From injections that spared LPC, there was little anterograde labeling in PM, but rather many fibers of passage and terminals in the interstitial region between PM and PL, and some within the ventromedial tail of PL. The projection from nBOR was similar, but with a few fibers terminating in the contralateral pontine. Terminals from the TeO were sparse in PM, but PL was heavily labeled. As the Wulst, GLv, and LM are all topographically organized (Funke, 1989; Gamlin & Cohen, 1988b; Wylie et al., 2009) and our injections did not cover

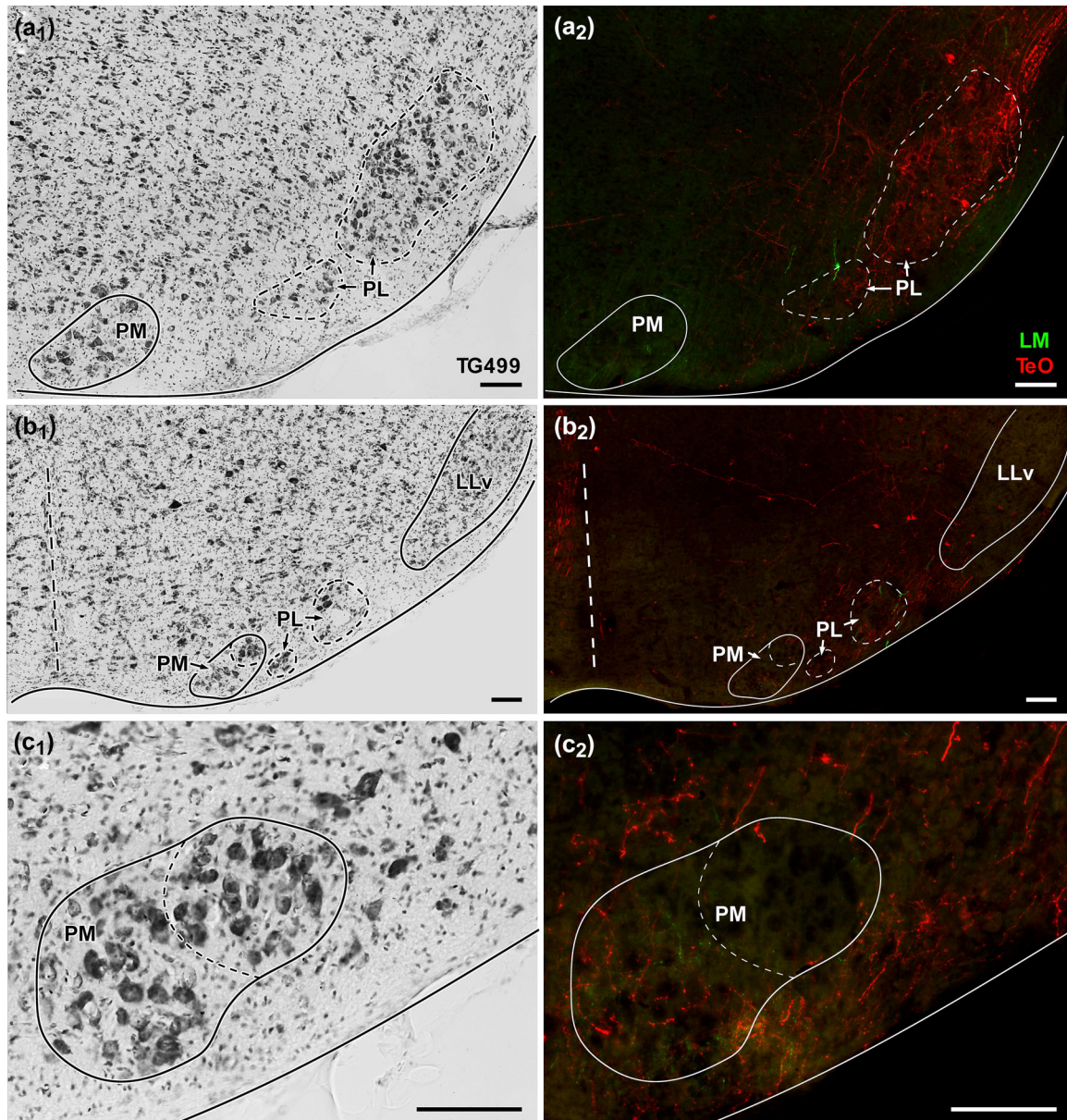


**FIGURE 8** Divisions of the medial and lateral pontine nuclei (PM and PL) and anterograde terminal labeling from the optic tectum (TeO). (a<sub>1</sub>) Nissl-stained mid-anterioposterior coronal sections through the pontine nuclei revealed two divisions of the PL indicated with dashed lines. (a<sub>2</sub>) The corresponding fluorescent photomicrograph shows a strong projection from the TeO to the lateral division of PL but not PM. Lentiformis mesencephali (LM) terminals are visible in PM but not PL, with a few LM fibers passing through the medial division of PL. (b<sub>1</sub>) Nissl-stained section posterior to section in panel (a<sub>1</sub>). (b<sub>1</sub> and b<sub>2</sub>) The divisions of PL are smaller; anterogradely labeled LM and TeO terminals target the medial subdivision of PM, with some TeO fibers with terminals entering the lateral subdivision of PM. Anterogradely labeled TeO terminals target both divisions of PL. Vertical dashed lines indicate the midline. (c<sub>1</sub> and c<sub>2</sub>) A high magnification photomicrograph of PM showing distribution of LM and TeO terminals. Scale bars = 100  $\mu$ m.

the entirety of these neuronal structures, it is possible that they each have a topographic projection to the pontine nuclei that is both more extensive and more detailed than we describe.

#### 4.1 | Comparison with previous work

The majority of the projections to the pontine nuclei described in this study for the zebra finch have been previously reported in pigeons

but the topography of these projections has not been described. Previous studies in pigeons have shown that TeO projects to PL and the surrounding reticular formation (Hunt & Künzle, 1976). We found a similar projection from TeO to the ipsilateral PL and adjacent reticular formation in the zebra finch, particularly to rostral levels of PL (Figures 8 and 9). However, we also observed a projection to PM, which has not been described in pigeons, although this projection is not as strong as that to PL (Figures 8 and 9). We found that in the zebra finch, GLv projects heavily to the ipsilateral PM (Figures 6c–e), similar to that

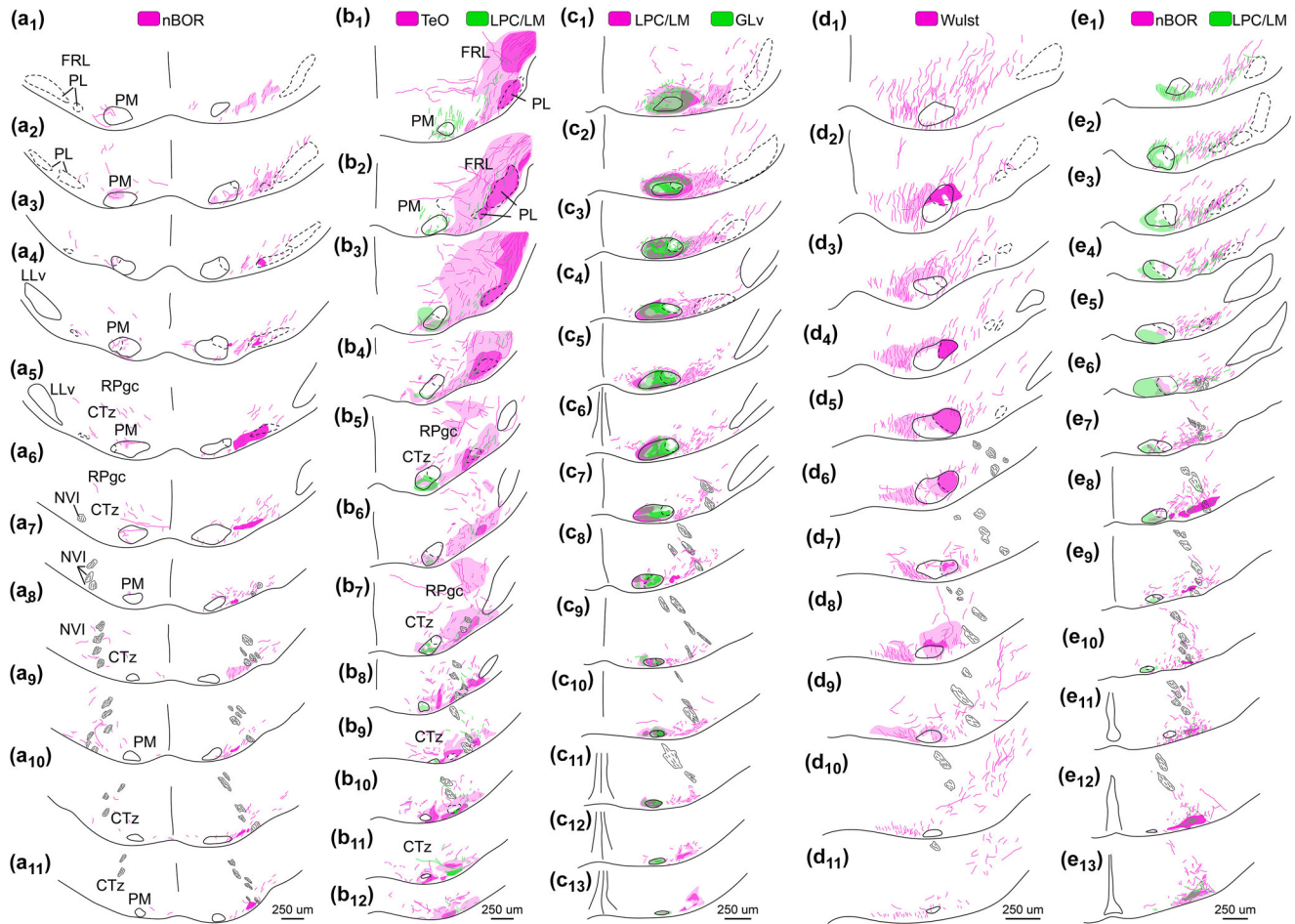


**FIGURE 9** A summary of the projections and fibers from the nucleus of the basal optic root (nBOR), the pretectal including both the nucleus laminaris precommissuralis and nucleus lentiformis mesencephali (LPC/LM), optic tectum (TeO), ventral lateral geniculate nucleus (GLv), and the somatosensory anterior Wulst to the medial and lateral pontine nuclei (PM and PL). Injection site and corresponding color are indicated at the top of each series of sections. (a–e) Drawings of the PM and PL anterior (top) to posterior (bottom) are based on Nissl-stained sections from the case indicated at the top. Darkly shaded regions indicate intense terminal labeling. Lines indicate fibers. Panel (a) shows bilateral projections from an injection in the right nBOR (TG497). Panel (b) illustrates ipsilateral labeling from injections in the TeO (magenta) and LPC/LM (green) from case TG499. Panel (c) illustrates ipsilateral labeling from injections in the LPC/LM (magenta) and GLv (green) from case TG505. Panel (d) shows ipsilateral labeling from an injection in the somatosensory anterior Wulst (TG511), and panel (e) shows ipsilateral labeling from injections in the nBOR (magenta) and LPC/LM (green) from case TG513. The subdivisions of PM are visible and indicated by a dashed line. It is also visible in each case where the PL separates into separate divisions; the PL is outlined in dashed lines. NVI, sixth cranial nerve; LLv, lateral lemniscus, ventral nucleus; Dpt, descending pretectal tract. Scale bars = 250  $\mu$ m.

described in pigeons (Marín et al., 2001). From our injections in GLv, it is also clear that in the zebra finch GLv receives a topographic projection from a subpopulation of neurons in layer 10 of the TeO, similar to that in chickens and pigeons (Figure 5c; Vega-Zuniga et al., 2014). In the case of nBOR, our results are also similar to those reported for pigeons (Wylie et al., 1997), where a small and bilateral projection to both PM and PL had been reported. Regarding LM, previous work in pigeons using retrograde tracers injected in the medial pontine area had found a projection from the LPC but not LM (Gamlin & Cohen, 1988a). Concordantly, in the zebra finch we found projections from LM to PM only when the injection included LPC, and not when the injections were exclusively in LM (Figures 3–7). In pigeons, injections of anterograde tracers in LM have suggested that LM also projects to

PL (Clarke, 1977; Gamlin & Cohen, 1988a; Pakan et al., 2006). A previous study found no evidence of a projection from LM to PL in zebra finches (Wild & Gaede, 2016). In this study, we show that fibers originating in LM traverse the medial most tip of PL and leave some en passant synapses (Figure 7), although most terminals are in the interstitial area between PM and PL and not in PL proper (Figures 6, 7, and 9).

Finally, our results confirm the projection from the anterior Wulst to PM in zebra finches (Wild & Williams, 2000). Interestingly, the projections from the anterior Wulst to PM nuclei is not found in all birds. It is present in zebra finches (this study; Wild & Williams, 2000), ravens (*Corvus corax*) (Adamo, 1967), Owls (little owl, *Athene cunicularia*, (Karten, 1971)), and Parrots (Adamo, 1967; Zecha, 1962) but is not

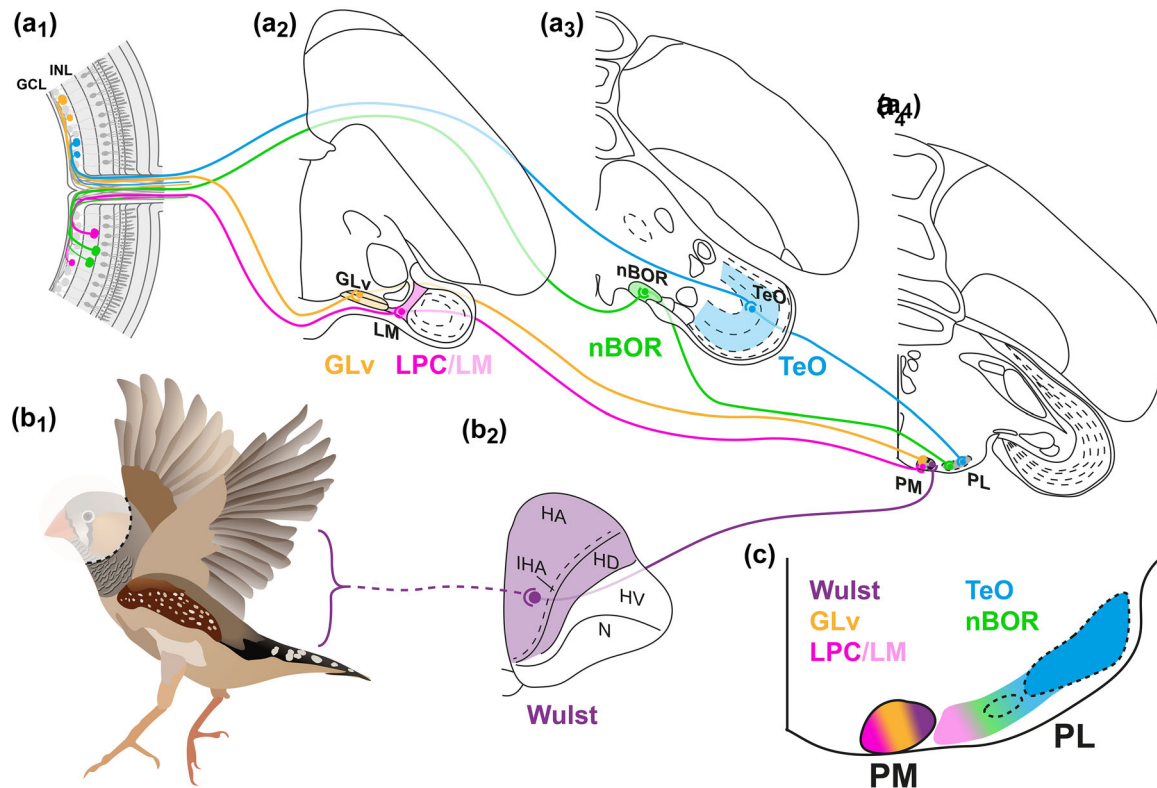


**FIGURE 10** Overview illustration of projections highlighted in this study, which originate in visual and somatosensory brain regions and terminate in the medial and lateral pontine nuclei (PM and PL). From the retina, both retinal ganglion cells (RGCs) and displaced ganglion cells (DGCs) project to the lentiform mesencephali (LM; magenta). The nucleus of the basal optic root (nBOR; green) primarily receives projections from the DGCs. The ventral lateral geniculate nucleus (GLv; yellow) and optic tectum (TeO; blue) both receive projections from the RGCs. The nucleus laminaris precommisuralis (LPC), which is immediately medial to LM, is also retinal-recipient (Gamlin & Cohen, 1988b). These four visual regions project to the pontine nuclei, with the PM receiving primary input from the GLv and LM and the PL receiving inputs from the TeO and nBOR. The anterior Wulst is a somatosensory region of the anterior telencephalon that has a representation of the body, excluding the beak. The anterior Wulst strongly projects to the PM. The inset highlights the areas of the PM and PL with the densest projections from the indicated brain regions.

present in chickens (*Gallus gallus*) (Adamo, 1967) or pigeons (Gutiérrez-Ibáñez et al., 2018). Recently, Gutiérrez-Ibáñez et al. (2023) showed that skilled foot-use has evolved repeatedly among birds, but almost exclusively after the emergence of Telluraves (core landbirds) about 65 million years ago (Gutiérrez-Ibáñez et al., 2023). Zebra finches, ravens, owls and parrots are all Telluraves, whereas chickens and pigeons are not. The anterior Wulst has a heavy representation of the hindlimbs (Manger et al., 2002; Wild, 2015). We speculate that the novel projection from the anterior Wulst to PM evolved to support skilled foot use among Telluraves.

#### 4.2 | Visual integration in the pontine nuclei of birds

We have previously suggested that the integration of local motion (from the TeO) and optic flow information (from LM/nBOR) in the brain of birds may be implicated in “steering” to avoid obstacles during locomotion through cluttered environments (Elder et al., 2009; Page & Duffy, 2008; Wylie et al., 2018). Given the direct projection from LM to

the oculomotor cerebellum (Gamlin & Cohen, 1988a; Gutiérrez-Ibáñez et al., 2022; Pakan & Wylie, 2006) and the projections from TeO to PL, which then also projects to the oculomotor cerebellum (Clarke, 1977; Gutiérrez-Ibáñez et al., 2022; Hunt & Künzle, 1976), we have previously argued this could happen in the cerebellum. Nonetheless, because previous studies suggested a projection from LM to PL (see above), we suspected this could be an earlier site of integration of the two types of visual inputs. Surprisingly, we found very few inputs from LM to PL or PM, and conclude that in the zebra finch the pretectal projection to PM arises from LPC, as it has been shown in pigeons (Gamlin & Cohen, 1988a). Although little is known about the function of LPC in birds, in chickens, cells in LPC have been shown to have large dendritic trees that lie in the adjacent LMm, so it is possible that they respond to optic flow like LM cells, but this is unclear. Therefore, at least at the level of the pontine nuclei, there is little integration between optic flow inputs from LM and local motion inputs from TeO. Interestingly, we show here that LPC and GLv project to adjacent but overlapping regions of PM (Figures 6c–e and 9c<sub>1–9</sub>). Additionally, this area receives small inputs from TeO and nBOR, which respond to local motion and optic flow respectively (Bilge, 1971; Cronly-Dillon, 1964;

Frost, 1978; Frost et al., 1990; Frost & DiFranco, 1976; Gianni et al., 1984; Winterson & Brauth, 1985). While the functional role of GLv in visual processing remains unclear (Gianni et al., 1991; Guiloff et al., 1987; Vega-Zuniga et al., 2016), GLv receives a strong topographic input from TeO (Gamlin & Cohen, 1988a; Guiloff et al., 1987; Karten et al., 1973; Vega-Zuniga et al., 2014, 2016; Wylie et al., 2009), and therefore is likely to also respond to local motion. Therefore, it is possible that some integration of local motion and optic flow happens in PM, but this is rather between LPC and GLv and not TeO and LM as was suggested by previous studies. Interestingly, Vega-Zuniga et al. (2016, 2018) showed that in the chicken, LPC receives inputs directly from GLv, further suggesting that these two nuclei form part of the same visual processing network.

### 4.3 | Multisensory integration in PM

Visual information from two different structures (LPC and GLv) as well as somatosensory information from the anterior Wulst are organized topographically in PM. Particularly, we show that somatosensory and visual information are largely separated in two subdivisions of PM, although there could be some overlap (Figure 9). This suggests that, at least at the level of the pontine nuclei, these two sensory streams may not be strongly integrated. Nonetheless, somatosensory-visual integration is expected during flight. Somatosensory receptors among the feathers detect changes in airflow (Brown & Fedde, 1993), which could encode aerodynamic features such as stall, lift, airspeed, and so on, and thus play a critical role in flight control (Altshuler et al., 2015). Given the role of visual inputs in the control of flight, particularly optic flow (Altshuler & Srinivasan, 2018; Dakin et al., 2016; Goller & Altshuler, 2014; Wylie et al., 2018), one would expect somatosensory and visual inputs to be integrated, this is possible in PM, but there is little overlap between the inputs of the Wulst and those from GLv, TeO, and LPC. Therefore, it is likely that this integration occurs in the oculomotor cerebellum. This separation between tactile and visual areas in the pontine nuclei of birds is similar to what has been found in mammals where visual and somatosensory inputs from the cortex are organized in separate clusters and neurons (Schwarz et al., 2005).

### 4.4 | Zonal organization of pontocerebellar inputs

Recently, Gutierrez-Ibanez et al. (2022) showed that in pigeons, projections from the pontine nuclei to the oculomotor cerebellum follow the same parasagittal zones as IO inputs and cerebellar nuclei outputs (Arends & Zeigler, 1991; Arends & Voogd, 1989; Gutierrez-Ibanez et al., 2022). In particular, they showed that the PL sends bilateral projections to the most medial part of the oculomotor cerebellum, zone A1, as well as to the most lateral zone, E. The PM, in contrast, sends largely contralateral projections to zones A2 and C. Projections from PM and PL are therefore segregated in the oculomotor cerebellum. This, combined with the segregation of inputs found in this study between PL and PM, means that parallel and independent sensorimotor pathways

exist in the oculomotor cerebellum of birds. Zone A1 receives visual inputs from the tectofugal pathway, either through the PL or from inputs of the visual arcopallium to the lateral SpM, which also projects to zone A1 (Gutiérrez-Ibáñez et al., 2022). Alternatively, Zones A2 and C receive inputs from GLv, LM, and anterior Wulst through the PM. This zone receives additional input from the anterior Wulst via the medial subdivision of the SpM, which receives inputs from the anterior Wulst (Wild & Williams, 2000). Interestingly, the results from Gutierrez-Ibanez et al. (2022) for pigeons also suggest that outputs from PM could be further segregated in the oculomotor cerebellum. These authors showed that zone A2 receives inputs from a lateral and dorsal area of PM whereas zone C received input from the surrounding PM, a pattern that closely resembles the segregation of anterior Wulst and LPC/GLv inputs in the PM of the zebra finch showed here (Figures 5 and 6). This arrangement means that zone A2 may receive stronger inputs from anterior Wulst, whereas zone C may receive stronger inputs from GLv and LM. Given that these zones in the oculomotor cerebellum project to different cerebellar nuclei or areas (Arends & Zeigler, 1991), these inputs are segregated in the outputs of the cerebellum. What the functional significance of these parallel pathways is remains unknown, but in the past we have argued that the medial pathway that involves PL-zone A1 and the medial cerebellar nuclei is more involved in feedforward control of locomotion, and the pathway between PM-zone A2/C and the lateral cerebellar nuclei is involved more in feedback control of movements (Gutiérrez-Ibáñez et al., 2022).

### 4.5 | Comparison with mammals

The pontine nuclei of mammals receives diverse cortical and subcortical inputs, which resemble those of birds to some degree. The superior colliculus (homologous to the TeO), GLv, and NOT (homologous to LM) have all been shown to project to the pontine nuclei in mammals (Kratowil et al., 2017; Ramnani, 2006). Additionally, most regions of the cortex project to the pontine nuclei (Henschke & Pakan, 2020; Kratowil et al., 2017; Ramnani, 2006; Wu et al., 2023). In birds, both the Wulst and arcopallium, the two main outputs of the pallium, project to the pontine nuclei; however, it is unclear whether the projections from the pallium to the pontine nuclei in birds are as widespread as in mammals. For example, PM receives projections from the somatosensory Wulst (homologous to S1/M1), but no projections from the more posterior visual Wulst (homologous to the V1 of mammals) have been reported (Karten, 1971; Miceli et al., 1987). In contrast, V1 sends projections to pontine nuclei in rodents (Henschke & Pakan, 2020; Kratowil et al., 2017). The pontine nuclei of mammals also receive projections from the prefrontal/associative areas (Henschke & Pakan, 2020; Kratowil et al., 2017). In birds, the nidopallium caudolaterale (NCL), which is analogous to the prefrontal cortex of mammals (Waldmann & Güntürkün, 1993), projects to the arcopallium (Kröner & Güntürkün, 1999), which then sends projections to PL (Fernández et al., 2020; Zeier & Karten, 1971). Therefore, some connectivity between associative areas and pontine nuclei is possible; however, more detailed studies are needed.

Our results showed segregation of different pallial and subpallial inputs to the pontine nuclei of birds. This is similar to what has been observed in mammals, where several studies have shown that cortical and subcortical inputs are clearly segregated in the pontine nuclei (reviewed in Kratochwil et al., 2017). This means that not only are the inputs to the pontine nuclei similar between birds and mammals, but that it is organized in a similar fashion. The pontine nuclei of birds and mammals have been proposed to be homologous (Brodal et al., 1950), but the fact that reptiles lack pontine nuclei, including alligators, the closest relatives to birds, makes this unclear (Bangma & Donkelaar, 1982; Gutiérrez-Ibáñez et al., 2022; Schwarz, & Schwarz, 1980). If the pontine nuclei of birds and mammals are not homologous, the similar organization of these inputs in these two groups would imply an impressive case of convergent evolution, one that suggests that similar computations have evolved in the cerebellum of birds and mammals.

## 5 | CONCLUSION

Our results show that projections carrying global optic flow, local “object” motion, and somatosensory information are topographically organized in the pontine nuclei of the zebra finch. We have previously shown that the medial column of the zebra finch IO is organized into several distinct subnuclei that are differentially targeted by mid-brain visual motion processing nuclei. Together, these data add to the growing collection of evidence suggesting that species-specific specializations exist in the neural pathways carrying optic flow information in birds (Gaede et al., 2017, 2019, 2022; Smyth et al., 2022; Wylie et al., 2023). Specializations in how visual motion data is communicated and processed may be related to the ecological demands and flight behavior of different species. Zebra finches perform flap-bounding flight, typically feed on the ground, and live in grassy woodland habitats where they may come in close contact with a variety of foliage common to arid environments. They also have a high wingbeat frequency and are able to perform rapid flight maneuvers, which places high demands on the visuomotor system (Tobalske et al., 1999, 2005). Furthermore, a high degree of parcellation within brain structures is an indicator of system specialization (Cloutman & Lambon Ralph, 2012; Ebbesson, 1984). Further study examining the functional role of the subdivisions and topography of the pontine nuclei is required, particularly within the context of optic flow and local motion integration.

## AUTHOR CONTRIBUTION

All authors had full access to all the data in the study and take responsibility for the integrity of the data and the accuracy of the data analysis. Study concept and design: C. G.-I., A. H. G., and D. R. W. Performed experiments and processed tissue: A. H. G., P.-H. W., and C. G.-I. Microscopy and image acquisition: M. P., C. G.-I., and P.-H. W. Data analysis: C. G.-I., A. H. G., and D. R. W. Drafting of the article: A. H. G., C. G.-I., and D. R. W. Construction of figures: D. R. W., C. G.-I., and A. H. G. Critical revision of the article for important intellectual content: D. L. A. Obtained funding: D. L. A. and D. R. W. Student supervision: D. L. A., D. R. W., C. G.-I., and A. H. G.

## ACKNOWLEDGMENTS

This research was supported by funding to D. R. W. and D. L. A. from the Natural Sciences and Engineering Research Council of Canada (NSERC) and the Canadian Institute for Health Research (CIHR).

## CONFLICT OF INTEREST STATEMENT

The authors have no conflict of interest.

## DATA AVAILABILITY STATEMENT

The data and images that support the findings of this study are available from the corresponding authors upon request.

## ORCID

Andrea H. Gaede  <https://orcid.org/0000-0002-1909-7004>

Cristián Gutiérrez-Ibáñez  <https://orcid.org/0000-0002-0468-8223>

Pei-Hsuan Wu  <https://orcid.org/0000-0001-8147-6083>

Douglas L. Altshuler  <https://orcid.org/0000-0002-1364-3617>

Douglas R. Wylie  <https://orcid.org/0000-0003-0782-1146>

## PEER REVIEW

The peer review history for this article is available at <https://publons.com/publon/10.1002/cne.25556>.

## REFERENCES

- Adamo, N. J. (1967). Connections of efferent fibers from hyperstriatal areas in chicken, raven, and African lovebird. *Journal of Comparative Neurology*, 131, 337–355. <https://doi.org/10.1002/cne.901310304>
- Altshuler, D. L., Bahlman, J. W., Dakin, R., Gaede, A. H., Goller, B., Lentink, D., Segre, P. S., & Skandalis, D. A. (2015). The biophysics of bird flight: functional relationships integrate aerodynamics, morphology, kinematics, muscles, and sensors. *Canadian Journal of Zoology*, 93, 961–975. <https://doi.org/10.1139/cjz-2015-0103>
- Altshuler, D. L., & Srinivasan, M. V. (2018). Comparison of visually guided flight in insects and birds. *Frontiers in neuroscience*, 12, 157. <https://doi.org/10.3389/fnins.2018.00157>
- Arends, J. J. A., & Zeigler, H. P. (1991). Organization of the cerebellum in the pigeon (*Columba livia*): I. Corticonuclear and corticovestibular connections. *Journal of Comparative Neurology*, 306, 221–244. <https://doi.org/10.1002/cne.903060203>
- Arends, J. J. A., & Voogd, J. (1989). Topographical aspects of the olivocerebellar system in the pigeon. *Exp Brain Res Suppl*, 17, 52–57.
- Bangma, G. C., & Donkelaar, H. J. T. (1982). Afferent connections of the cerebellum in various types of reptiles. *Journal of Comparative Neurology*, 207, 255–273. <https://doi.org/10.1002/cne.902070306>
- Bilge, M. (1971). Electrophysiological investigations on the pigeon's optic tectum. *Quarterly Journal of Experimental Physiology and Cognate Medical Sciences*, 56, 242–249. <https://doi.org/10.1113/expphysiol.1971.sp002125>
- Biswas, M. S., Luo, Y., Sarpong, G. A., & Sugihara, I. (2019). Divergent projections of single pontocerebellar axons to multiple cerebellar lobules in the mouse. *Journal of Comparative Neurology*, 527, 1966–1985. <https://doi.org/10.1002/cne.24662>
- Brauth, S E., & Olds, J. (1977). Direct accessory optic projections to the vestibulo-cerebellum: A possible channel for oculomotor control systems. *Experimental Brain Research*, 134, 73–82. [https://doi.org/10.1016/0006-8993\(77\)90926-X](https://doi.org/10.1016/0006-8993(77)90926-X)
- Brecha, N., & Karten, H. J. (1979). Accessory optic projections upon oculomotor nuclei and vestibulocerebellum. *Science*, 203, 913–916. <https://doi.org/10.1126/science.570303>



- Brecha, N., Karten, H. J., & Hunt, S. P. (1980). Projections of the nucleus of the basal optic root in the pigeon: An autoradiographic and horseradish peroxidase study. *Journal of Comparative Neurology*, 189, 615–670. <https://doi.org/10.1002/cne.901890404>
- Brodal, A., Kristiansen, K., & Jansen, J. (1950). Experimental demonstration of a pontine homologue in birds. *Journal of Comparative Neurology*, 92, 23–69. <https://doi.org/10.1002/cne.900920104>
- Brown, R. E., & Fedde, M. R. (1993). Airflow sensors in the avian wing. *Journal of Experimental Biology*, 179, 13–30. <https://doi.org/10.1242/jeb.179.1.13>
- Clarke, P. G. H. (1977). Some visual and other connections to the cerebellum of the pigeon. *Journal of Comparative Neurology*, 174, 535–552. <https://doi.org/10.1002/cne.901740307>
- Cloutman, L. L., & Lambon Ralph, M. A. (2012). Connectivity-based structural and functional parcellation of the human cortex using diffusion imaging and tractography. *Front Neuroanat*, 6, 34. <https://doi.org/10.3389/fnana.2012.00034>
- Cronly-Dillon, J. R. (1964). Units sensitive to direction of movement in goldfish optic tectum. *Nature*, 203, 214–215. <https://doi.org/10.1038/203214a0>
- Dakin, R., Fellows, T. K., & Altshuler, D. L. (2016). Visual guidance of forward flight in hummingbirds reveals control based on image features instead of pattern velocity. *Proceedings National Academy of Science USA*, 113, 8849–8854. <https://doi.org/10.1073/pnas.1603221113>
- Dubbeldam, J. L., Den Boer-Visser, A. M., & Bout, R. G. (1997). Organization and efferent connections of the archistriatum of the mallard, *Anas platyrhynchos* L.: An anterograde and retrograde tracing study. *Journal of Comparative Neurology*, 388, 632–657. [https://doi.org/10.1002/\(SICI\)1096-9861\(19971201\)388:4%3c632::AID-CNE10%3e3.0.CO;2-N](https://doi.org/10.1002/(SICI)1096-9861(19971201)388:4%3c632::AID-CNE10%3e3.0.CO;2-N)
- Ebbesson, S. O. E. (1984). Evolution and ontogeny of neural circuits. *Behavioral and Brain Sciences*, 7, 321–331. <https://doi.org/10.1017/S0140525X00018379>
- Elder, D. M., Grossberg, S., & Mingolla, E. (2009). A neural model of visually guided steering, obstacle avoidance, and route selection. *Journal of Experimental Psychology: Human Perception and Performance*, 35, 1501–1531. <https://doi.org/10.1037/a0016459>
- Faunes, M., Fernández, S., Gutiérrez-Ibáñez, C., Iwaniuk, A. N., Wylie, D. R., Mpodozis, J., Karten, H. J., & Marín, G. (2013). Laminar segregation of GABAergic neurons in the avian nucleus isthmi pars magnocellularis: A retrograde tracer and comparative study: The Avian Nucleus Isthmi Magnocellularis. *Journal of Comparative Neurology*, 521, 1727–1742. <https://doi.org/10.1002/cne.23253>
- Fernández, M., Morales, C., Durán, E., Fernández-Colleman, S., Sentsis, E., Mpodozis, J., Karten, H. J., & Marín, G. J. (2020). Parallel organization of the avian sensorimotor arcopallium: Tectofugal visual pathway in the pigeon (*Columba livia*). *Journal of Comparative Neurology*, 528, 597–623. <https://doi.org/10.1002/cne.24775>
- Frost, B. J. (1978). Moving background patterns alter directionally specific responses of pigeon tectal neurons. *Brain Research*, 151, 599–603. [https://doi.org/10.1016/0006-8993\(78\)91093-4](https://doi.org/10.1016/0006-8993(78)91093-4)
- Frost, B. J., & Difranco, D. E. (1976). Motion characteristics of single units in the pigeon optic tectum. *Vision Research*, 16, 1229–1234. [https://doi.org/10.1016/0042-6989\(76\)90046-8](https://doi.org/10.1016/0042-6989(76)90046-8)
- Frost, B. J., Wylie, D. R., & Wang, Y.-C. (1990). The processing of object and self-motion in the tectofugal and accessory optic pathways of birds. *Vision Research*, 30, 1677–1688. [https://doi.org/10.1016/0042-6989\(90\)90152-B](https://doi.org/10.1016/0042-6989(90)90152-B)
- Funke, K. (1989). Somatosensory areas in the telencephalon of the pigeon. *Experimental Brain Research*, 76, 620–638. <https://doi.org/10.1007/BF00248918>
- Gaede, A. H., Baliga, V. B., Smyth, G., Gutiérrez-Ibáñez, C., Altshuler, D. L., & Wylie, D. R. (2022). Response properties of optic flow neurons in the accessory optic system of hummingbirds versus zebra finches and pigeons. *Journal of Neurophysiology*, 127, 130–144. <https://doi.org/10.1152/jn.00437.2021>
- Gaede, A. H., Goller, B., Lam, J. P. M., Wylie, D. R., & Altshuler, D. L. (2017). Neurons responsive to global visual motion have unique tuning properties in hummingbirds. *Current Biology*, 27, 279–285. <https://doi.org/10.1016/j.cub.2016.11.041>
- Gaede, A. H., Gutierrez-Ibanez, C., Armstrong, M. S., Altshuler, D. L., & Wylie, D. R. (2019). Pretectal projections to the oculomotor cerebellum in hummingbirds (*Calypte anna*), zebra finches (*Taeniopygia guttata*), and pigeons (*Columba livia*). *Journal of Comparative Neurology*, 527, 2644–2658. <https://doi.org/10.1002/cne.24697>
- Gamlin, P. D. R., & Cohen, D. H. (1988a). Projections of the retinorecipient pretectal nuclei in the pigeon (*Columba livia*). *Journal of Comparative Neurology*, 269, 18–46. <https://doi.org/10.1002/cne.902690103>
- Gamlin, P. D. R., & Cohen, D. H. (1988b). Retinal projections to the pretectum in the pigeon (*Columba livia*). *Journal of Comparative Neurology*, 269, 1–17. <https://doi.org/10.1002/cne.902690102>
- Gamlin, P. D. R., Reiner, A., Keyser, K. T., Brecha, N., & Karten, H. J. (1996). Projection of the nucleus pretectalis to a retinorecipient tectal layer in the pigeon (*Columba livia*). *Journal of Comparative Neurology*, 368, 424–438. [https://doi.org/10.1002/\(SICI\)1096-9861\(19960506\)368:3%3c424::AID-CNE8%3e3.0.CO;2-7](https://doi.org/10.1002/(SICI)1096-9861(19960506)368:3%3c424::AID-CNE8%3e3.0.CO;2-7)
- Gioanni, H., Palacios, A., Sansonetti, A., & Varela, F. (1991). Role of the nucleus geniculatus lateralis ventralis (GLv) in the optokinetic reflex: a lesion study in the pigeon. *Experimental Brain Research*, 86, 601–607. <https://doi.org/10.1007/BF00230533>
- Gioanni, H., Rey, J., Villalobos, J., & Dalbera, A. (1984). Single unit activity in the nucleus of the basal optic root (nBOR) during optokinetic, vestibular and visuo-vestibular stimulations in the alert pigeon (*Columba livia*). *Experimental Brain Research*, 57, 49–60. <https://doi.org/10.1007/BF00231131>
- Giolli, R. A., Gregory, K. M., Suzuki, D. A., Blanks, R. H. I., Lui, F., & Betelak, K. F. (2001). Cortical and subcortical afferents to the nucleus reticularis tegmenti pontis and basal pontine nuclei in the macaque monkey. *Visual Neuroscience*, 18, 725–740. <https://doi.org/10.1017/S0952523801185068>
- Goller, B., & Altshuler, D. L. (2014). Hummingbirds control hovering flight by stabilizing visual motion. *Proceedings National Academy of Science USA*, 111, 18375–18380. <https://doi.org/10.1073/pnas.1415975111>
- Guiloff, G. D., Maturana, H. R., & Varela, F. J. (1987). Cytoarchitecture of the avian ventral lateral geniculate nucleus. *Journal of Comparative Neurology*, 264, 509–526. <https://doi.org/10.1002/cne.902640406>
- Guo, J.-Z., Sauerbrei, B. A., Cohen, J. D., Mischiati, M., Graves, A. R., Pisanello, F., Branson, K. M., & Hantman, A. W. (2021). Disrupting cortico-cerebellar communication impairs dexterity. *Elife*, 10, e65906. <https://doi.org/10.7554/eLife.65906>
- Gutiérrez-Ibáñez, C., Amaral-Peçanha, C., Iwaniuk, A. N., Wylie, D. R., & Baron, J. (2023). Online repositories of photographs and videos provide insights into the evolution of skilled hindlimb movements in birds. *Communications Biology*, 6, 781. <https://doi.org/10.1038/s42003-023-05151-z>
- Gutierrez-Ibanez, C., Fernandez, M. D., Marin, G. J., & Wylie, D. R. (2018). Organization of telencephalic inputs to the medial spiriform nucleus, a pretectal cerebellar relay nucleus in birds. Society for Neuroscience Annual Meeting.
- Gutierrez-Ibanez, C., Gaede, A. H., Dannish, M. R., Altshuler, D. L., & Wylie, D. R. (2018). The retinal projection to the nucleus lentiformis mesencephali in zebra finch (*Taeniopygia guttata*) and Anna's hummingbird (*Calypte anna*). *Journal of Comparative Physiology A*, 204, 369–376. <https://doi.org/10.1007/s00359-018-1245-5>
- Gutiérrez-Ibáñez, C., Kettler, L., Pilon, M. C., Carr, C. E., & Wylie, D. R. (2023b). Cerebellar inputs in the American alligator (*Alligator mississippiensis*). *Brain Behav E*, 98, 44–60. <https://doi.org/10.1159/000527348>
- Gutiérrez-Ibáñez, C., Pilon, M. C., & Wylie, D. R. (2022). Pretecto- and ponto-cerebellar pathways to the pigeon oculomotor cerebellum follow a zonal organization. *Journal of Comparative Neurology*, 530, 817–833. <https://doi.org/10.1002/cne.25247>

- Hellmann, B., & Güntürkün, O. (2001). Structural organization of parallel information processing within the tectofugal visual system of the pigeon. *Journal of Comparative Neurology*, 429, 94–112. [https://doi.org/10.1002/1096-9861\(2000101\)429:1%3c94::AID-CNE8%3e3.0.CO;2-5](https://doi.org/10.1002/1096-9861(2000101)429:1%3c94::AID-CNE8%3e3.0.CO;2-5)
- Henschke, J. U., & Pakan, J. M. (2020). Disynaptic cerebocerebellar pathways originating from multiple functionally distinct cortical areas. *Elife*, 9, e59148. <https://doi.org/10.7554/eLife.59148>
- Hunt, S. P., & Künzle, H. (1976). Observations on the projections and intrinsic organization of the pigeon optic tectum: An autoradiographic study based on anterograde and retrograde, axonal and dendritic flow. *Journal of Comparative Neurology*, 170, 153–172. <https://doi.org/10.1002/cne.901700203>
- Karten, H. J. (1971). Efferent projections of the wulst of the owl. *Anatomical Record*, 169, 353–353.
- Karten, H. J., & Hodos, W. (1967). *A stereotaxic atlas of the brain of the pigeon: (Columba livia)*. Johns Hopkins Press.
- Karten, H. J., Hodos, W., Nauta, W. J. H., & Revzin, A. M. (1973). Neural connections of the “visual wulst” of the avian telencephalon. Experimental studies in the pigeon (*Columba livia*) and owl (*Speotyto cunicularia*). *Journal of Comparative Neurology*, 150, 253–277. <https://doi.org/10.1002/cne.901500303>
- Kratochwil, C. F., Maheshwari, U., & Rijli, F. M. (2017). The long journey of pontine nuclei neurons: From rhombic lip to cortico-ponto-cerebellar circuitry. *Front Neural Circuits*, 11, 33. <https://doi.org/10.3389/fncir.2017.00033>
- Kröner, S., & Güntürkün, O. (1999). Afferent and efferent connections of the caudolateral neostriatum in the pigeon (*Columba livia*): a retro- and anterograde pathway tracing study. *Journal of Comparative Neurology*, 407, 228–260. [https://doi.org/10.1002/\(SICI\)1096-9861\(19990503\)407:2%3c228::AID-CNE6%3e3.0.CO;2-2](https://doi.org/10.1002/(SICI)1096-9861(19990503)407:2%3c228::AID-CNE6%3e3.0.CO;2-2)
- Leergaard, T. B. (2007). Topography of the complete corticopontine projection: From experiments to principal maps. *Frontiers in neuroscience*, 1, 211–223. <https://doi.org/10.3389/neuro.01.1.1.016.2007>
- Luksch, H. (2003). Cytoarchitecture of the avian optic tectum: neuronal substrate for cellular computation. *Reviews in the Neurosciences*, 14, 85–106. <https://doi.org/10.1515/REVNEURO.2003.14.1-2.85>
- Manger, P. R., Elston, G. N., & Pettigrew, J. D. (2002). Multiple maps and activity-dependent representational plasticity in the anterior Wulst of the adult barn owl (*Tyto alba*): Somatosensory Wulst of the owl. *European Journal of Neuroscience*, 16, 743–750. <https://doi.org/10.1046/j.1460-9568.2002.02119.x>
- Marín, G., Henny, P., Letelier, J. C., Sentis, E., Karten, H., Mrosko, B., & Mpodozis, J. (2001). A simple method to microinject solid neural tracers into deep structures of the brain. *Journal of Neuroscience Methods*, 106, 121–129. [https://doi.org/10.1016/S0165-0270\(01\)00332-6](https://doi.org/10.1016/S0165-0270(01)00332-6)
- Miceli, D., Repérant, J., Villalobos, J., & Dionne, L. (1987). Extratelencephalic projections of the avian visual Wulst. A quantitative autoradiographic study in the pigeon *Columba livia*. *Journal Fur Hirnforschung*, 28, 45–57.
- Nagao, S. (2004). Pontine nuclei-mediated cerebello-cerebral interactions and its functional role. *Cerebellum (London, England)*, 3, 11–15. <https://doi.org/10.1080/14734220310012181>
- Page, W. K., & Duffy, C. J. (2008). Cortical neuronal responses to optic flow are shaped by visual strategies for steering. *Cerebral Cortex*, 18, 727–739. <https://doi.org/10.1093/cercor/bhm109>
- Pakan, J. M. P., Graham, D. J., & Wylie, D. R. (2010). Organization of visual mossy fiber projections and zebrin expression in the pigeon vestibulo-cerebellum. *Journal of Comparative Neurology*, 518, 175–198. <https://doi.org/10.1002/cne.22192>
- Pakan, J. M. P., Krueger, K., Kelcher, E., Cooper, S., Todd, K. G., & Wylie, D. R. W. (2006). Projections of the nucleus lentiformis mesencephali in pigeons (*Columba livia*): A comparison of the morphology and distribution of neurons with different efferent projections. *Journal of Comparative Neurology*, 495, 84–99. <https://doi.org/10.1002/cne.20855>
- Pakan, J. M. P., & Wylie, D. R. W. (2006). Two optic flow pathways from the pretectal nucleus lentiformis mesencephali to the cerebellum in pigeons (*Columba livia*). *Journal of Comparative Neurology*, 499, 732–744. <https://doi.org/10.1002/cne.21108>
- Ramnani, N. (2006). The primate cortico-cerebellar system: anatomy and function. *Nature Reviews Neuroscience*, 7, 511–522. <https://doi.org/10.1038/nrn1953>
- Reiner, A., & Karten, H. J. (1982). Laminar distribution of the cells of origin of the descending tectofugal pathways in the pigeon (*Columba livia*). *Journal of Comparative Neurology*, 204, 165–187. <https://doi.org/10.1002/cne.902040206>
- Schneider, A., & Necker, R. (1996). Electrophysiological investigations of the somatosensory thalamus of the pigeon. *Experimental Brain Research*, 109, 377–383. <https://doi.org/10.1007/BF00229621>
- Schwarz, C., Horowski, A., Möck, M., & Thier, P. (2005). Organization of tectopontine terminals within the pontine nuclei of the rat and their spatial relationship to terminals from the visual and somatosensory cortex. *Journal of Comparative Neurology*, 484, 283–298. <https://doi.org/10.1002/cne.20461>
- Schwarz, I. E., & Schwarz, D. W. F. (1980). Afferents to the cerebellar cortex of turtles studied by means of the horseradish peroxidase technique. *Anat Embryol*, 160, 39–52. <https://doi.org/10.1007/BF00315648>
- Smyth, G., Baliga, V. B., Gaede, A. H., Wylie, D. R., & Altshuler, D. L. (2022). Specializations in optic flow encoding in the pretectum of hummingbirds and zebra finches. *Current Biology*, S0960982222007126.
- Tobalske, B. W., Peacock, W. L., & Dial, K. P. (1999). Kinematics of flap-bounding flight in the zebra finch over a wide range of speeds. *Journal of Experimental Biology*, 202, 1725–1739. <https://doi.org/10.1242/jeb.202.13.1725>
- Tobalske, B. W., Puccinelli, L. A., & Sheridan, D. C. (2005). Contractile activity of the pectoralis in the zebra finch according to mode and velocity of flap-bounding flight. *Journal of Experimental Biology*, 208, 2895–2901. <https://doi.org/10.1242/jeb.01734>
- Vega-Zuniga, T., Marín, G., González-Cabrera, C., Planitscher, E., Hartmann, A., Marks, V., Mpodozis, J., & Luksch, H. (2016). Microconnectomics of the pretectum and ventral thalamus in the chicken (*Gallus gallus*): Microconnectomics in the chicken. *Journal of Comparative Neurology*, 524, 2208–2229. <https://doi.org/10.1002/cne.23941>
- Vega-Zuniga, T., Mpodozis, J., Karten, H. J., Marín, G., Hain, S., & Luksch, H. (2014). Morphology, projection pattern, and neurochemical identity of Cajal’s “centrifugal neurons”: The cells of origin of the tectoventrogeniculate pathway in pigeon (*Columba livia*) and chicken (*Gallus gallus*). *Journal of Comparative Neurology*, 522, 2377–2396. <https://doi.org/10.1002/cne.23539>
- Waldmann, C., & Güntürkün, O. (1993). The dopaminergic innervation of the pigeon caudolateral forebrain: Immunocytochemical evidence for a ‘pre-frontal cortex’ in birds? *Brain Research*, 600, 225–234. [https://doi.org/10.1016/0006-8993\(93\)91377-5](https://doi.org/10.1016/0006-8993(93)91377-5)
- Wang, Y., Luksch, H., Brecha, N. C., & Karten, H. J. (2006). Columnar projections from the cholinergic nucleus isthmi to the optic tectum in chicks (*Gallus gallus*): A possible substrate for synchronizing tectal channels. *Journal of Comparative Neurology*, 494, 7–35. <https://doi.org/10.1002/cne.20821>
- Wild, J. M. (1987). The avian somatosensory system: Connections of regions of body representation in the forebrain of the pigeon. *Brain Research*, 412, 205–223. [https://doi.org/10.1016/0006-8993\(87\)91127-9](https://doi.org/10.1016/0006-8993(87)91127-9)
- Wild, J. M. (1997). The avian somatosensory system: The pathway from wing to Wulst in a passerine *Chloris chloris*. *Brain Research*, 759, 122–134. [https://doi.org/10.1016/S0006-8993\(97\)00253-9](https://doi.org/10.1016/S0006-8993(97)00253-9)
- Wild, J. M. (2015). Chapter 5 - The avian somatosensory system: A comparative view. In: *Sturkie’s Avian Physiology (Sixth Edition)*, edited by Scanes CG. San Diego: Academic Press, p. 55–69. <https://doi.org/10.1016/B978-0-12-407160-5.00005-1>
- Wild, J. M., & Gaede, A. H. (2016). Second tectofugal pathway in a songbird (*Taeniopygia guttata*) revisited: Tectal and lateral pontine projections to

- the posterior thalamus, thence to the intermediate nidopallium: Second Tectofugal Pathway in a Songbird. *Journal of Comparative Neurology*, 524, 963–985. <https://doi.org/10.1002/cne.23886>
- Wild, J. M., Kubke, M. F., & Peña, J. L. (2008). A pathway for predation in the brain of the barn owl (*Tyto alba*): Projections of the gracile nucleus to the “claw area” of the rostral wulst via the dorsal thalamus. *Journal of Comparative Neurology*, 509, 156–166. <https://doi.org/10.1002/cne.21731>
- Wild, J. M., & Williams, M. N. (2000). Rostral Wulst in passerine birds. I. Origin, course, and terminations of an avian pyramidal tract. *Journal of Comparative Neurology*, 416, 429–450. [https://doi.org/10.1002/\(SICI\)1096-9861\(20000124\)416:4%3c429::AID-CNE2%3e3.0.CO;2-X](https://doi.org/10.1002/(SICI)1096-9861(20000124)416:4%3c429::AID-CNE2%3e3.0.CO;2-X)
- Winterson, B. J., & Brauth, S. E. (1985). Direction-selective single units in the nucleus lentiformis mesencephali of the pigeon (*Columba livia*). *Experimental Brain Research*, 60, 215–226. <https://doi.org/10.1007/BF00235916>
- Wu, X., Sarpong, G. A., Zhang, J., & Sugihara, I. (2023). Divergent topographic projection of cerebral cortical areas to overlapping cerebellar lobules through distinct regions of the pontine nuclei. *Heliyon*, 9, e14352. <https://doi.org/10.1016/j.heliyon.2023.e14352>
- Wylie, D. R., Gaede, A. H., Gutiérrez-Ibáñez, C., Wu, P.-H., Pilon, M. C., Azargoon, S., & Altshuler, D. L. (2023). Topography of optic flow processing in olivo-cerebellar pathways in zebra finches (*Taeniopygia guttata*). *Journal of Comparative Neurology*, 531, 640–662. <https://doi.org/10.1002/cne.25454>
- Wylie, D. R., Gutiérrez-Ibáñez, C., Gaede, A. H., Altshuler, D. L., & Iwaniuk, A. N. (2018). Visual-cerebellar pathways and their roles in the control of avian flight. *Frontiers in neuroscience*, 12, 223. <https://doi.org/10.3389/fnins.2018.00223>
- Wylie, D. R. W., Gutierrez-Ibanez, C., Pakan, J. M. P., & Iwaniuk, A. N. (2009). The optic tectum of birds: Mapping our way to understanding visual processing. *Canadian Journal of Experimental Psychology*, 63, 328–338. <https://doi.org/10.1037/a0016826>
- Wylie, D. R. W., Linkenhoker, B., & Lau, K. L. (1997). Projections of the nucleus of the basal optic root in pigeons (*Columba livia*) revealed with biotinylated dextran amine. *Journal of Comparative Neurology*, 384, 517–536. [https://doi.org/10.1002/\(SICI\)1096-9861\(19970811\)384:4%3c517::AID-CNE3%3e3.0.CO;2-5](https://doi.org/10.1002/(SICI)1096-9861(19970811)384:4%3c517::AID-CNE3%3e3.0.CO;2-5)
- Zecha, A. (1962). The “pyramidal tract” and other telencephalic efferents in birds. *Acta Morphologica Neerlando-Scandinavica*, 5, 194–195.
- Zeier, H., & Karten, H. J. (1971). The archistriatum of the pigeon: organization of afferent and efferent connections. *Brain Research*, 31, 313–326. [https://doi.org/10.1016/0006-8993\(71\)90185-5](https://doi.org/10.1016/0006-8993(71)90185-5)

**How to cite this article:** Gaede, A. H., Gutiérrez-Ibáñez, C., Wu, P.-H., Pilon, M. C., Altshuler, D. L., & Wylie, D. R. (2023). Topography of visual and somatosensory inputs to the pontine nuclei in zebra finches (*Taeniopygia guttata*). *Journal of Comparative Neurology*, 1–19. <https://doi.org/10.1002/cne.25556>